

A Class of Stabilizing Controllers for Flexible Multibody Systems

Suresh M. Joshi, Atul G. Kelkar, and Peiman G. Maghami



A Class of Stabilizing Controllers for Flexible Multibody Systems

Suresh M. Joshi, Atul G. Kelkar, and Peiman G. Maghami
Langley Research Center • Hampton, Virginia

Abstract

This paper considers the problem of controlling a class of nonlinear multibody flexible space systems consisting of a flexible central body to which a number of articulated appendages are attached. Collocated actuators and sensors are assumed, and global asymptotic stability of such systems is established under a nonlinear dissipative control law. The stability is shown to be robust to unmodeled dynamics and parametric uncertainties. For a special case in which the attitude motion of the central body is small, the system, although still nonlinear, is shown to be stabilized by linear dissipative control laws. Two types of linear controllers are considered: static dissipative (constant gain) and dynamic dissipative. The static dissipative control law is also shown to provide robust stability in the presence of certain classes of actuator and sensor nonlinearities and actuator dynamics. The results obtained for this special case can also be readily applied for controlling single-body linear flexible space structures. For this case, a synthesis technique for the design of a suboptimal dynamic dissipative controller is also presented. The results obtained in this paper are applicable to a broad class of multibody and single-body systems such as flexible multilink manipulators, multipayload space platforms, and space antennas. The stability proofs use the Lyapunov approach and exploit the inherent passivity of such systems.

1. Introduction

A class of spacecraft envisioned for the future will require flexible multibody systems such as space platforms with multiple articulated payloads and space-based manipulators used for satellite assembly and servicing. Examples of such systems include the Earth Observing System (EOS) and Upper Atmospheric Research Satellite (UARS). (See refs. 1 and 2, respectively.) These systems are expected to have significant flexibility in their structural members as well as joints. Control system design for such systems is a difficult problem because of the highly nonlinear dynamics, large number of significant elastic modes with low inherent damping, and uncertainties in the mathematical model. The published literature contains a number of important stability results for some subclasses of this problem (e.g., linear flexible structures, nonlinear multibody rigid structures, and most recently, multibody flexible structures). Under certain conditions, the input-output maps for such systems can be shown to be passive. (See ref. 3.) The Lyapunov and passivity approaches are used in reference 4 to demonstrate global asymptotic stability (g.a.s.) of linear flexible space structures (with no articulated appendages) for a class of dissipative compensators. The stability properties were shown to be robust to first-order actuator dynamics and certain actuator-sensor nonlinearities. Multibody rigid structures represent another class of systems for which stability results have been advanced. Subject to a few restrictions, these systems can be ideally categorized as natural systems. (See ref. 5.) Such systems are known to exhibit global asymptotic stability under proportional-and-derivative (PD) control. After recognition that rigid manipulators belong to the class of natural systems, a number of researchers (refs. 6–9) established global asymptotic stability of terrestrial rigid manipulators by using PD control with gravity compensation. Stability of tracking controllers was investigated in references 10 and 11 for rigid manipulators. In reference 12, the results of reference 11 were extended to accomplish exponentially stable tracking control of flexible

multilink manipulators local to the desired trajectory. Lyapunov stability of multilink flexible systems was addressed in reference 13. However, the global asymptotic stability of nonlinear, multilink, flexible space structures, which to date has not been addressed in the literature, is the principal subject of this paper.

The structure to be considered is a complete nonlinear rotational dynamic model of a multibody flexible spacecraft which is assumed to have a branched geometry, (i.e., a central flexible body with various flexible appendage bodies). (See fig. 1.) Throughout this paper, actuators and sensors are assumed to be collocated. Global asymptotic stability of such systems controlled by a nonlinear dissipative controller is proved. In many applications, the central body has large mass and moments of inertia when compared with that of the appendage bodies. As a result, the motion of the central body is small and can be considered to be in the linear range. For this case, robust stability is proved with linear static as well as with linear dynamic dissipative compensators. The effects of realistic nonlinearities in the actuators and sensors are also investigated. The stability proofs use Lyapunov's method (ref. 9) and LaSalle's theorem. For systems with linear collocated actuators and sensors, the stability proof by Lyapunov's method can take a simpler form if the work-energy rate principle (ref. 13) is used. However, because the work-energy rate principle is applicable only when the system is holonomic and scleronomic in nature, a more direct approach is used here in evaluating the time derivative of the Lyapunov function which makes the results more general.

The organization of the paper is as follows. In section 3, a nonlinear mathematical model of a generic flexible multibody system is given. A special property of the system, which is pivotal to the proofs, and some basic kinematic relations of the quaternion (i.e., measure of attitude of the central body) are given. Section 4 establishes the global asymptotic stability of the complete nonlinear system under a nonlinear control law based on quaternion feedback. A special case, in which the central body attitude motion is small, is considered in section 5. Global asymptotic stability is proved under static dissipative compensation, and these results are extended to the case in which certain actuator and sensor nonlinearities are present. In addition, dynamic dissipative compensators, a more versatile class of dissipative compensators, are considered. Section 6 presents the application of the results to the important special case of linear single-body spacecraft. Two numerical examples are given in section 7 and some concluding remarks are given in section 8.

2. Symbols

A	system matrix
\tilde{A}	diagonal matrix (eq. (79))
B	control influence matrix
\tilde{B}	diagonal matrix (eq. (80))
C	Coriolis and centrifugal force coefficient matrix
\tilde{C}	diagonal matrix of squares of eigenvalues
D	damping matrix
\tilde{D}	structural damping matrix
E	Euler transformation matrix; modulus of elasticity
F	compensator output matrix
$G(s), G'(s)$	plant transfer function

$G_{Ai}(s)$	actuator transfer function
G_a	acceleration gain matrix
G_p, \overline{G}_p	position gain matrices
G_r	rate gain matrix
H	estimator gain matrix
I_k	$k \times k$ identity matrix
i	index variable
J	inertia matrix of single-body spacecraft
\mathcal{J}	performance index
j	index variable
K	stiffness matrix of system
\hat{K}	stiffness matrix of system for linear case
\tilde{K}	stiffness matrix for flexible degrees of freedom
$\mathcal{K}(s)$	controller transfer function
k	number of rigid body degrees of freedom
L	Lagrangian of system
L_{2e}^k	extended Lebesgue space
$M(p)$	mass-inertia matrix of system
\widehat{M}	mass-inertia matrix of system for linear case
n	number of total degrees of freedom
n_q	number of flexible degrees of freedom
P	Lyapunov matrix
p, \hat{p}	generalized coordinate vectors
\tilde{p}	vector of rigid body coordinates
Q_p, Q_r	output weighting matrices
q	vector of flexural coordinates
R	control weighting matrix
S	skew-symmetric matrix
\mathcal{S}	property of the system
s	Laplace variable
T	terminal time; kinetic energy
$T(s)$	transfer matrix
u	vector of control input
V	Lyapunov function candidate
v	integrator output

x, \bar{x}	state vectors
y_a	acceleration output
y_p	position output
y_r	rate output
z	state vector
α	the quaternion
$\hat{\alpha}_i$	i th component of unit vector along eigenaxis
$\bar{\alpha}$	vector part of quaternion
α_i	i th component of quaternion
β	scalar defined as $(\alpha_4 - 1)$
γ	integral of ω
Δ	transformation matrix
δ	performance function
ζ	state vector
η	Euler angle vector
θ	vector of rotational degrees of freedom between rigid bodies
Λ	diagonal matrix (eq. (82))
μ	scalar gain
ν	input to nonlinearity
ξ	state vector
ρ_i	damping in i th structural mode
ς	controller state vector
Φ	mode shape matrix
ϕ	Euler rotation
φ	defined as $-\theta$
ψ_{ai}	actuator nonlinearity (i th loop)
ψ_{pi}	position sensor nonlinearity (i th loop)
ψ_{ri}	rate sensor nonlinearity (i th loop)
Ω	cross product operator of vector ω
ω	angular velocity vector for central body

Abbreviations:

a.s.	asymptotically stable
DDC	dynamic dissipative controller
EOS	Earth Observing System
g.a.s.	globally asymptotically stable

LQG	linear quadratic Gaussian
MSPR	marginally strictly positive-real
PD	proportional and derivative
PR	positive-real
SPR	strictly positive-real
UARS	Upper Atmospheric Research Satellite

3. Mathematical Model

3.1. Equations of Motion

The class of systems considered herein consists of a branched configuration of flexible bodies as shown in figure 1. Each branch by itself could be a serial chain of structures. For the sake of simplicity and without loss of generality, consider a spacecraft with only one such branch where each appendage body has one degree of freedom (hinge joint) with respect to the previous body in the chain. The results presented in this paper are also applicable to the general case with multiple branches. Consider the spacecraft consisting of a central flexible body and a chain of $(k - 3)$ flexible links. The central body has three rigid rotational degrees of freedom, and each link is connected by one rotational degree of freedom to the neighboring link. The Lagrangian for this system can be shown (ref. 14) to have the following form:

$$L = \dot{p}^T M(p) \dot{p} - q^T \tilde{K} q \quad (1)$$

where $\dot{p} = (\omega^T, \dot{\theta}^T, \dot{q}^T)^T$, ω is the 3×1 inertial angular velocity vector (in body-fixed coordinates) for the central body, $\theta = (\theta_1, \theta_2, \dots, \theta_{(k-3)})^T$ (θ_i denotes the joint angle for the i th joint expressed in body-fixed coordinates), q is the $(n - k)$ vector of flexible degrees of freedom (modal amplitudes), $M(p) = M^T(p) > 0$ is the configuration-dependent mass-inertia matrix, and \tilde{K} is the symmetric positive-definite stiffness matrix related to the flexible degrees of freedom. From the Lagrangian equation (1), the following equations of motion are obtained:

$$M(p)\ddot{p} + C(p, \dot{p})\dot{p} + D\dot{p} + Kp = B^T u \quad (2)$$

where $p = (\gamma^T, \theta^T, q^T)^T$, $\dot{\gamma} = \omega$, $C(p, \dot{p})$ corresponds to Coriolis and centrifugal forces, D is the symmetric positive-semidefinite damping matrix, $B = [I_{k \times k} \quad 0_{k \times (n-k)}]$ is the control influence matrix, and u is the k vector of applied torques. The first three components of u represent the attitude control torques applied to the central body about its X -, Y -, and Z -axes; the remaining components are the torques applied at the $(k - 3)$ joints. The symmetric positive-semidefinite stiffness and damping matrices K and D are

$$K = \begin{bmatrix} 0_{k \times k} & 0_{k \times (n-k)} \\ 0_{(n-k) \times k} & \tilde{K}_{(n-k) \times (n-k)} \end{bmatrix} \quad D = \begin{bmatrix} 0_{k \times k} & 0_{k \times (n-k)} \\ 0_{(n-k) \times k} & \tilde{D}_{(n-k) \times (n-k)} \end{bmatrix} \quad (3)$$

where \tilde{K} and \tilde{D} are symmetric positive-definite. The details of the derivation of the mathematical model can be found in reference 14; a summary is provided in the appendix.

The angular measurements for the central body are Euler angles (not the vector γ), whereas the remaining angular measurements between bodies are relative angles. One important inherent property of such systems that is crucial to the stability results presented in this paper is defined next.

Property S: The matrix $(\frac{1}{2}\dot{M} - C)$ is skew-symmetric for the system represented by equation (2). The justification of this property is given by theorem A1 in the appendix.

The central-body attitude (Euler angle) vector η is given by $E(\eta)\dot{\eta} = \omega$, where $E(\eta)$ is a 3×3 transformation matrix. (See ref. 15.) The sensor outputs consist of three central-body Euler angles, the $(k - 3)$ joint angles, and the angular rates (i.e., the sensors are collocated with the torque actuators). The sensor outputs are then given by

$$y_p = B\hat{p} \quad y_r = B\dot{p} \quad (4)$$

where $\hat{p} = (\eta^T, \theta^T, q^T)^T$ and η is the Euler angle vector for the central body. The measured angular position and rate vectors are $y_p = (\eta^T, \theta^T)^T$ and $y_r = (\omega^T, \dot{\theta}^T)^T$, respectively. The body rate measurements ω are assumed to be available from rate gyros. The input-output map from u to y_r is passive as shown in theorem A2 of the appendix.

3.2. Quaternion as Measure of Attitude

The orientation of a free-floating body can be minimally represented by a three-dimensional orientation vector. However, this representation is not unique. Euler angles are commonly used as a minimal representation of the attitude. As stated previously, the 3×1 Euler angle vector η is given by $E(\eta)\dot{\eta} = \omega$, where $E(\eta)$ is a 3×3 transformation matrix. For certain values of η , $E(\eta)$ becomes singular; however, note that the limitations imposed on the allowable orientations because of this singularity are purely mathematical in nature and have no physical significance. The problem of singularity in the three-parameter representation of attitude has been studied in detail in the literature. An effective way of overcoming the singularity problem is to use the quaternion formulation. (See refs. 16–19.)

The unit quaternion (Euler parameter vector) α is defined as follows:

$$\alpha = (\bar{\alpha}^T, \alpha_4)^T \quad \bar{\alpha} = \begin{bmatrix} \hat{\alpha}_1 \\ \hat{\alpha}_2 \\ \hat{\alpha}_3 \end{bmatrix} \sin\left(\frac{\phi}{2}\right) \quad \alpha_4 = \cos\left(\frac{\phi}{2}\right) \quad (5)$$

where $\hat{\alpha} = (\hat{\alpha}_1, \hat{\alpha}_2, \hat{\alpha}_3)^T$ is the unit vector along the eigenaxis of rotation and ϕ is the magnitude of rotation. The quaternion is subject to the norm constraint

$$\bar{\alpha}^T \bar{\alpha} + \alpha_4^2 = 1 \quad (6)$$

The quaternion can also be shown (ref. 19) to obey the following kinematic differential equations:

$$\dot{\bar{\alpha}} = \frac{1}{2}(\omega \times \bar{\alpha} + \alpha_4 \omega) \quad (7)$$

$$\dot{\alpha}_4 = -\frac{1}{2}\omega^T \bar{\alpha} \quad (8)$$

The attitude control of a single-body rigid spacecraft with quaternion feedback has been thoroughly investigated in references 16–19. The quaternion representation is used here for the central-body attitude. The quaternion can be computed from Euler angle measurements given by equations (4). (See ref. 20.)

The open-loop system, given by equations (2), (7), and (8), has multiple equilibrium solutions $(\bar{\alpha}_{ss}^T, \alpha_{4ss}, \theta_{ss}^T)^T$, where the subscript ss denotes the steady-state value; the steady-state value

of q is zero. By defining $\beta = (\alpha_4 - 1)$ and denoting $\dot{p} = z$, equations (2), (7), and (8) can be rewritten as

$$M\dot{z} + Cz + Dz + \tilde{K}q = B^T u \quad (9a)$$

$$\begin{bmatrix} \dot{\theta} \\ \dot{q} \end{bmatrix} = \begin{bmatrix} 0_{(n-3) \times 3} & I_{(n-3) \times (n-3)} \end{bmatrix} z \quad (9b)$$

$$\dot{\bar{\alpha}} = \frac{1}{2}[\omega \times \bar{\alpha} + (\beta + 1)\omega] \quad (10)$$

$$\dot{\beta} = -\frac{1}{2}\omega^T \bar{\alpha} \quad (11)$$

In equation (9a) the matrices M and C are functions of p and (p, \dot{p}) , respectively. Note that the first three elements of p associated with the orientation of the central body can be fully described by the unit quaternion. Hence, M and C are implicit functions of α , and therefore the system represented by equations (9)–(11) is time-invariant and can be expressed in the state-space form as follows:

$$\dot{x} = f(x, u) \quad (12)$$

where $x = (\bar{\alpha}^T, \beta, \theta^T, q^T, z^T)^T$. Note that the dimension of x is $(2n + 1)$, which is one more than the dimension of the system in equation (2). However, the constraint of equation (6) is now present. Verification that the constraint of equation (6) is satisfied for all $t > 0$ if it is satisfied at $t = 0$ easily follows from equations (7) and (8).

4. Nonlinear Dissipative Control Law

Consider the dissipative control law u , given by

$$u = -G_p \tilde{p} - G_r y_r \quad (13)$$

where $\tilde{p} = (\bar{\alpha}^T, \theta^T)^T$. Matrices G_p and G_r are symmetric positive-definite $k \times k$ matrices; G_p is given by

$$G_p = \begin{bmatrix} \left(1 + \frac{(\beta+1)}{2}\right)G_{p1} & 0_{3 \times (k-3)} \\ 0_{(k-3) \times 3} & G_{p2(k-3) \times (k-3)} \end{bmatrix} \quad (14)$$

Note that equations (13) and (14) represent a nonlinear control law. If G_p and G_r satisfy certain conditions, this control law can be shown to render the time rate of change of the system's energy negative along all trajectories (i.e., it is a *dissipative* control law).

The closed-loop equilibrium solution can be obtained by equating all the derivatives to zero in equations (2), (10), and (11). In particular, $\dot{p} = \ddot{p} = 0 \Rightarrow \omega = 0, \dot{\theta} = 0, \dot{q} = 0$, and

$$-B^T G_p \tilde{p} = \begin{bmatrix} -G_p \tilde{p} \\ 0_{(n-k) \times 1} \end{bmatrix} = \begin{bmatrix} 0_{k \times 1} \\ \tilde{K}q \end{bmatrix} \quad (15)$$

Because of equation (6), $|\beta + 1| \leq 1$. Therefore G_p is positive-definite and equation (15) implies $\tilde{p} = (\bar{\alpha}^T, \theta^T)^T = 0$ and $q = 0$. The equilibrium solution of equation (11) is $\beta = \beta_{ss} = \text{Constant}$ (i.e., $\alpha_4 = \text{Constant}$), which implies from equation (6) that $\alpha_4 = \pm 1$. Thus, there appear to be two closed-loop equilibrium points corresponding to $\alpha_4 = 1$ and $\alpha_4 = -1$ (all other state variables are zero). However, from equations (5), $\alpha_4 = 1 \Rightarrow \phi = 0$, and $\alpha_4 = -1 \Rightarrow \phi = 2\pi$ (i.e., only one equilibrium point exists in the physical space).

One of the objectives of the control law is to transfer the state of the system from one orientation (i.e., equilibrium position) to another orientation. Without loss of generality, the target

orientation can be defined to be zero, and the initial orientation, given by $(\bar{\alpha}(0), \alpha_4(0), \theta(0))$, can always be defined in such a way that $|\phi_i(0)| \leq \pi$, $0 \leq \alpha_4(0) \leq 1$ (corresponds to $|\phi| \leq \pi$), and $(\bar{\alpha}(0), \alpha_4(0))$ satisfy equation (6).

The following theorem establishes the global asymptotic stability of the physical equilibrium state of the system.

Theorem 1: Suppose $G_{p2(k-3) \times (k-3)}$ and $G_{r_{k \times k}}$ are symmetric and positive-definite, and $G_{p1} = \mu I_3$, where $\mu > 0$. Then, the closed-loop system given by equations (12) and (13) is globally asymptotically stable (g.a.s.).

Proof: Consider the candidate Lyapunov function

$$V = \frac{1}{2} \dot{p}^T M(p) \dot{p} + \frac{1}{2} q^T \tilde{K} q + \frac{1}{2} \theta^T G_{p2} \theta + \frac{1}{2} \bar{\alpha}^T (G_{p1} + 2\mu I_3) \bar{\alpha} + \mu \beta^2 \quad (16)$$

Here, V is clearly positive-definite and radially unbounded with respect to a state vector $(\bar{\alpha}^T, \beta, \theta^T, q^T, \dot{p}^T)^T$ because $M(p)$, \tilde{K} , G_{p1} , and G_{p2} are all positive-definite symmetric matrices. Note that the matrix $M(p)$, although configuration dependent, is uniformly bounded from below and above by the values which correspond to the minimum and maximum inertia configurations, respectively (i.e., there exist positive-definite matrices \underline{M} and \overline{M} such that $\underline{M} \leq M \leq \overline{M}$). The time derivative of V results in

$$\dot{V} = \dot{p}^T M \ddot{p} + \frac{1}{2} \dot{p}^T \dot{M} \dot{p} + \dot{q}^T \tilde{K} q + \dot{\theta}^T G_{p2} \theta + \dot{\bar{\alpha}}^T (G_{p1} + 2\mu I_3) \bar{\alpha} + 2\beta \dot{\beta} \mu \quad (17)$$

With the use of equations (2), (4), (10), (11), and (14),

$$\begin{aligned} \dot{V} = & \dot{p}^T B^T u + \dot{p}^T \left(\frac{1}{2} \dot{M} - C \right) \dot{p} - \dot{p}^T D \dot{p} - \dot{p}^T K p + \dot{q}^T \tilde{K} q + \dot{\theta}^T G_{p2} \theta \\ & + \frac{1}{2} (\Omega \bar{\alpha})^T G_{p1} \bar{\alpha} + \frac{1}{2} (\beta + 1) \omega^T G_{p1} \bar{\alpha} + \mu \omega^T \bar{\alpha} \end{aligned} \quad (18)$$

where $\Omega = (\omega \times)$ denotes the skew-symmetric cross product matrix (i.e., $\omega \times x = \Omega x$). With the substitution for u , the fact that $\dot{p}^T K p = \dot{q}^T \tilde{K} q$ and $(\Omega \bar{\alpha})^T G_{p1} \bar{\alpha} = 0$, and the use of property \mathcal{S} of the system, equation (18) becomes

$$\dot{V} = -\dot{p}^T \left(D + B^T G_r B \right) \dot{p} - (B \dot{p})^T G_p \tilde{p} + \frac{1}{2} (\beta + 1) \omega^T G_{p1} \bar{\alpha} + \mu \omega^T \bar{\alpha} + \dot{\theta}^T G_{p2} \theta \quad (19)$$

Note that $(B \dot{p})^T G_p \tilde{p} = \frac{1}{2} (\beta + 1) \omega^T G_{p1} \bar{\alpha} + \mu \omega^T \bar{\alpha} + \dot{\theta}^T G_{p2} \theta$. After several cancellations,

$$\dot{V} = -\dot{p}^T \left(D + B^T G_r B \right) \dot{p} \quad (20)$$

Because $(D + B^T G_r B)$ is a positive-definite symmetric matrix, $\dot{V} \leq 0$ (i.e., \dot{V} is negative-semidefinite) and $\dot{V} = 0 \Rightarrow \dot{p} = 0 \Rightarrow \ddot{p} = 0$. By substitution in the closed-loop equation, equation (15) results. As shown previously, equation (15) $\Rightarrow \tilde{p} = 0$ and $q = 0$; i.e., $\bar{\alpha} = 0$, $\theta = 0$, and $\alpha_4 = \pm 1$ (or $\beta = 0$ or -2). Consistent with the previous discussion, these values correspond to two equilibrium points representing the same physical equilibrium state.

From equation (16), verification easily follows that any small perturbation ϵ in α_4 from the equilibrium point corresponding to $\alpha_4 = -1$ will cause a decrease in the value of V ($\epsilon > 0$ because $|\alpha_4| \leq 1$). Thus, in the mathematical sense, $\alpha_4 = -1$ corresponds to an isolated equilibrium

point such that $\dot{V} = 0$ at that point and $\dot{V} < 0$ in the neighborhood of that point (i.e., $\alpha_4 = -1$ is a repeller and not an attractor). Previously, \dot{V} has been shown to be negative along all trajectories in the state space except at the two equilibrium points. That is, if the system's initial condition lies anywhere in the state space except at the equilibrium point corresponding to $\alpha_4 = -1$, then the system will asymptotically approach the origin (i.e., $x = 0$); if the system is at the equilibrium point corresponding to $\alpha_4 = -1$ at $t = 0$, then it will stay there for all $t > 0$. However, this is the same equilibrium point in the physical space; hence, by LaSalle's invariance theorem, the system is globally asymptotically stable. Q.E.D.

5. Systems in Attitude-Hold Configuration

Consider a special case where the central-body attitude motion is small. This can occur in many real situations. For example, in cases of space station-based or shuttle-based manipulators, the inertia of the base (central body) is much greater than that of any manipulator link or payload. In such cases, the rotational motion of the base can be assumed to be in the linear region, although the payloads (or links) attached to it can undergo large rotational and translational motions and nonlinear dynamic loading because of Coriolis and centripetal accelerations. The attitude of the central body is simply γ (the integral of the inertial angular velocity ω) and the use of quaternions is not necessary. The equations of motion (2) can now be expressed in the state-space form simply as

$$\dot{\bar{x}} = \begin{bmatrix} 0 & I \\ -M^{-1}K & -M^{-1}(C + D) \end{bmatrix} \bar{x} + \begin{bmatrix} 0 \\ B^T \end{bmatrix} u \quad (21)$$

where $\bar{x} = (p^T, \dot{p}^T)^T$, $p = (\gamma^T, \theta^T, q^T)^T$, and M and C are functions of \bar{x} .

5.1. Stability With Static Dissipative Controllers

The static dissipative control law u is given by

$$u = -\bar{G}_p y_p - G_r y_r \quad (22)$$

where \bar{G}_p is symmetric positive-definite $k \times k$ matrix and

$$y_p = Bp \quad y_r = B\dot{p} \quad (23)$$

where y_p and y_r are measured angular position and rate vectors, respectively.

Theorem 2: Suppose $\bar{G}_{p_{k \times k}}$ and $G_{r_{k \times k}}$ are symmetric and positive-definite. Then, the closed-loop system given by equations (21)–(23) is globally asymptotically stable.

Proof: Consider the candidate Lyapunov function

$$V = \frac{1}{2} \dot{p}^T M(p) \dot{p} + \frac{1}{2} p^T (K + B^T \bar{G}_p B) p \quad (24)$$

Clearly, V is positive-definite because $M(p)$ and $(K + B^T \bar{G}_p B)$ are positive-definite symmetric matrices. Defining $\bar{K} = (K + B^T \bar{G}_p B)$, the time derivative of V can be shown to be

$$\dot{V} = \dot{p}^T \left(\frac{1}{2} \dot{M} - C \right) \dot{p} - \dot{p}^T \bar{K} p + \dot{p}^T \bar{K} p - \dot{p}^T (D + B^T G_r B) \dot{p} \quad (25)$$

Again, with the use of property \mathcal{S} , $\dot{p}^T (\frac{1}{2} \dot{M} - C) \dot{p} = 0$, and after some cancellations,

$$\dot{V} = -\dot{p}^T (D + B^T G_r B) \dot{p} \quad (26)$$

Because $(D + B^T G_r B)$ is a positive-definite matrix, $\dot{V} \leq 0$ (i.e., \dot{V} is negative-semidefinite in p and \dot{p} and $\dot{V} = 0 \Rightarrow \dot{p} = 0 \Rightarrow \ddot{p} = 0$). With substitution in the closed-loop equation (2) and u given by equation (22),

$$(K + B^T \overline{G}_p B)p = 0 \quad \Rightarrow p = 0 \quad (27)$$

Thus, \dot{V} is not zero along any trajectories; then, by LaSalle's theorem, the system is g.a.s. Q.E.D.

The significance of the two results presented in theorems 1 and 2 is that any nonlinear multibody system belonging to these classes can be robustly stabilized with the dissipative control laws given. In the case of manipulators, this means that any terminal angular position can be achieved from any initial position with guaranteed asymptotic stability.

5.2. Robustness to Actuator-Sensor Nonlinearities

Theorem 2, which assumes linear actuators and sensors, proves global asymptotic stability for systems in the attitude-hold configuration. In practice, however, the actuators and sensors have nonlinearities. The following theorem extends the results of reference 4 (pp. 59–62) to the case of nonlinear flexible multibody systems. That is, the robust stability property of the dissipative controller is proved to hold in the presence of a broad class of actuator-sensor nonlinearities with the following definition: a function $\psi(\nu)$ is said to belong to the $(0, \infty)$ sector (fig. 2(a)) if $\psi(0) = 0$ and $\nu\psi(\nu) > 0$ for $\nu \neq 0$ and ψ is said to belong to the $[0, \infty)$ sector if $\nu\psi(\nu) \geq 0$.

Let $\psi_{ai}(\cdot)$, $\psi_{pi}(\cdot)$, and $\psi_{ri}(\cdot)$ denote the nonlinearities in the i th actuator, position sensor, and rate sensor, respectively. Both \overline{G}_p and G_r are assumed to be diagonal with elements \overline{G}_{pi} and G_{ri} , respectively; then the actual input is given by

$$u_i = \psi_{ai}[-\overline{G}_{pi}\psi_{pi}(y_{pi}) - G_{ri}\psi_{ri}(y_{ri})] \quad (i = 1, 2, \dots, k) \quad (28)$$

With the assumption that ψ_{pi} , ψ_{ai} , and ψ_{ri} ($i = 1, 2, \dots, k$) are continuous single-valued functions, $R \rightarrow R$, the following theorem gives sufficient conditions for stability.

Theorem 3: Consider the closed-loop system given by equations (21), (23), and (28), where \overline{G}_p and G_r are diagonal with positive entries. Suppose ψ_{ai} , ψ_{pi} , and ψ_{ri} are single-valued, time-invariant continuous functions, and that (for $i = 1, 2, \dots, k$)

1. ψ_{ai} are monotonically nondecreasing and belong to the $(0, \infty)$ sector
2. ψ_{pi} and ψ_{ri} belong to the $(0, \infty)$ sector

Under these conditions, the closed-loop system is globally asymptotically stable.

Proof: (The proof closely follows that of ref. 4.) Let $\varphi = -y_p$ (k vector). Define

$$\overline{\psi}_{pi}(\nu) = -\psi_{pi}(-\nu) \quad (29)$$

$$\overline{\psi}_{ri}(\nu) = -\psi_{ri}(-\nu) \quad (30)$$

If ψ_{pi} , $\psi_{ri} \in (0, \infty)$ or $[0, \infty)$ sector, then $\overline{\psi}_{pi}$, $\overline{\psi}_{ri}$ also belong to the same sector. Now, consider the following Lur -Postnikov Lyapunov function:

$$V = \frac{1}{2}\dot{p}^T M(p)\dot{p} + \frac{1}{2}q^T \tilde{K} q + \sum_{i=1}^k \int_0^{\varphi_i} \psi_{ai}[\overline{G}_{pi}\overline{\psi}_{pi}(\nu)] d\nu \quad (31)$$

where \tilde{K} is the symmetric positive-definite part of K . Differentiation with respect to t and use of equation (2) yield

$$\dot{V} = \dot{p}^T (B^T u - C\dot{p} - D\dot{p} - Kp) + \frac{1}{2}\dot{p}^T \dot{M}\dot{p} + \sum_{i=1}^k \dot{\varphi}_i \psi_{ai} [\overline{G}_{pi} \overline{\psi}_{pi}(\varphi_i)] + \dot{q}^T \tilde{K} q \quad (32)$$

Upon several cancellations and the use of property \mathcal{S} ,

$$\dot{V} = \sum_{i=1}^k u_i y_{ri} - \dot{q}^T \tilde{D} \dot{q} + \sum_{i=1}^k \dot{\varphi}_i \psi_{ai} [\overline{G}_{pi} \overline{\psi}_{pi}(\varphi_i)] \quad (33)$$

where matrix \tilde{D} is the positive-definite part of D .

$$\dot{V} = -\dot{q}^T \tilde{D} \dot{q} - \sum_{i=1}^k \dot{\varphi}_i \{ \psi_{ai} [\overline{G}_{ri} \overline{\psi}_{ri}(\varphi_i)] + \overline{G}_{pi} \overline{\psi}_{pi}(\varphi_i) - \psi_{ai} [\overline{G}_{pi} \overline{\psi}_{pi}(\varphi_i)] \} \quad (34)$$

Because ψ_{ai} are monotonically nondecreasing and ψ_{ri} belong to the $(0, \infty)$ sector, $\dot{V} \leq 0$, and the system is at least Lyapunov-stable. In fact, it will be proved next that the system is g.a.s. First, consider a special case when ψ_{ai} are monotonically increasing. Then, $\dot{V} \leq -\dot{q}^T \tilde{D} \dot{q}$, and $\dot{V} = 0$ only when $\dot{q} = 0$ and $\dot{\varphi} = 0$, which implies $\dot{p} = 0 \Rightarrow \ddot{p} = 0$. Substitution in the closed-loop equation results in

$$Kp = B^T \psi_a [-\overline{G}_p \psi_p(y_p)] \quad (35)$$

$$\begin{bmatrix} 0 \\ \tilde{K} q \end{bmatrix} = \begin{bmatrix} \psi_a [-\overline{G}_p \psi_p(y_p)] \\ 0 \end{bmatrix} \quad (36)$$

$$\Rightarrow \psi_a [-\overline{G}_p \psi_p(y_p)] = 0 \quad \text{and} \quad q = 0$$

If ψ_{pi} belong to the $(0, \infty)$ sector, $\psi_{ai}(\nu) = \psi_{pi}(\nu) = 0$ only when $\nu = 0$. Therefore $y_p = 0$. Thus, $\dot{V} = 0$ only at the origin, and the system is g.a.s.

In the case when actuator nonlinearities are of the monotonically nondecreasing type (e.g., saturation nonlinearity), \dot{V} can be 0 even if $\dot{\varphi} \neq 0$. Figure 2(b) shows a monotonically nondecreasing nonlinearity. However, every system trajectory along which $\dot{V} \equiv 0$ will be shown to go to the origin asymptotically. When $\dot{\varphi} \neq 0$, $\dot{V} \equiv 0$ only when all actuators are locally saturated. Then, from the equations of motion, the system trajectories will go unbounded, which is not possible because the system was already proved to be Lyapunov-stable. Hence, \dot{V} cannot be identically zero along the system trajectories, and the system is g.a.s. **Q.E.D.**

For the case when the central-body motion is not in the linear range, the results of robust stability in the presence of actuator-sensor nonlinearities cannot be easily extended because the stabilizing control law given in equation (13) is nonlinear.

The next section extends the robust stability results of section 5.1 to a class of more versatile controllers called dynamic dissipative controllers. The advantages of using dynamic dissipative controllers include higher performance, more design freedom, and better noise attenuation.

5.3. Stability With Dynamic Dissipative Controllers

To obtain better performance without the loss of guaranteed robustness to unmodeled dynamics and parameter uncertainties, consider a class of dynamic dissipative controllers (DDC). Such compensators have been suggested in the past for controlling only the elastic motion

(refs. 21–23) of linear flexible space structures with no articulated appendages (i.e., single-body structures). These compensators were based on the fact that the plant, which consisted only of elastic modes with velocity measurements as the output, was passive (i.e., the transfer function was positive-real (PR)). A stability theorem based on Popov’s hyperstability concepts (ref. 24) was then used, which essentially states that a positive-real system controlled by a strictly positive-real (SPR) compensator is stable. Even in the linear single-body setting, certain problems occur with these results. In the first place, no attempt is made to control the rigid-body attitude, which is the main purpose of the control system. Secondly, the results assume that measurements of only the elastic motion are available and that the actuators affect only the elastic motion. These assumptions do not hold for real spacecraft unless the actuators are used in a balanced configuration for accomplishing only damping enhancement with no rigid-body control. (See ref. 4.) Finally, the stability theorem invoked assumes the compensator to be strictly positive-real, which is overly restrictive. It is also an ambiguous term having several nonequivalent definitions. (See ref. 25.) In view of these facts, the concept of marginally strictly positive-real (MSPR) systems will be introduced, which is stronger than the standard positive-real systems but is weaker than the weakly strictly positive-real systems defined in reference 25.

The results of this section address the problem of controlling both rigid and elastic modes; these results essentially extend and generalize the results of reference 26, which also addressed the control of rigid-plus-flexible modes, but only for the linear single-body case. In this section, the stability of dynamic dissipative compensators for flexible nonlinear multibody space structures in the attitude-hold configuration is proved by using some of the results and methods of reference 26.

5.3.1. Mathematical preliminaries. PR and MSPR systems are defined in definition 1 and definition 2, respectively.

Definition 1: A rational matrix-valued function $T(s)$ of the complex variable s is said to be positive-real if all of its elements are analytic in $\text{Re}[s] > 0$ and $T(s) + T^T(s^*) \geq 0$ in $\text{Re}[s] > 0$, where an asterisk (*) denotes the complex conjugate.

Scalar PR functions have a relative degree (i.e., the difference between the degrees of the denominator and numerator polynomials) of -1 , 0 , or 1 . (See ref. 27.) Positive-real matrices can be shown to have no transmission zeros or poles in the open right half of the complex plane, can have only simple poles on the imaginary axis with nonnegative definite residues. By application of the maximum modulus theorem, it is sufficient to check for positive-semidefiniteness of $T(s)$ only on the imaginary axis $s = j\omega$, $0 \leq \omega < \infty$; i.e., the condition becomes $T(j\omega) + T^*(j\omega) \geq 0$. Suppose $(\bar{A}, \bar{B}, \bar{C}, \bar{D})$ is an n th-order minimal realization of $T(s)$. From reference 28, a necessary and sufficient condition for $T(s)$ to be positive-real is that there exists an $n \times n$ symmetric positive-definite matrix P and matrices W and L such that

$$\left. \begin{aligned} \bar{A}^T P + P \bar{A} &= -L L^T \\ \bar{C} &= \bar{B}^T P + W^T L \\ W^T W &= \bar{D} + \bar{D}^T \end{aligned} \right\} \quad (37)$$

This result is generally known in the literature as the Kalman-Yakubovich lemma. A stronger concept along these lines is the SPR systems. However, as stated previously, there are several definitions of SPR systems. (See ref. 25.) The concept of weakly SPR (ref. 25) appears to be the least restrictive definition of SPR. Nevertheless, all the definitions of SPR seem to require the system to have all poles in the open left half plane.

The concept of marginally strictly PR systems is defined in reference 29 and included here in definition 2.

Definition 2: A rational matrix-valued function $T(s)$ of the complex variable s is said to be marginally strictly positive-real (MSPR) if $T(s)$ is PR and if $T(j\omega) + T^*(j\omega) > 0$ for $\omega \in (-\infty, \infty)$.

The obvious difference between this definition and the definition of PR systems is that the weak inequality (\geq) has been replaced by strict inequality. The difference between the MSPR and weak SPR of reference 25 is that the latter definition requires the system to have poles in the open left half plane, whereas the former definition permits poles on the $j\omega$ -axis. Reference 29 shows that an MSPR controller can robustly stabilize a PR plant.

5.3.2. Stability results. Consider the system given by equation (21) with the sensor outputs given by equations (23); then

$$y_p = (\gamma^T, \theta^T)^T \quad y_r = (\omega^T, \dot{\theta}^T)^T \quad (38)$$

where y_p and y_r are the measured angular position and rate vectors, respectively. The central-body attitude rate measurements ω are assumed to be available from rate gyros.

Suppose a controller $\mathcal{K}(s)$, with k inputs and k outputs, is represented by the minimal realization

$$\dot{x}_c = A_c x_c + B_c u_c \quad (39)$$

$$y_c = C_c x_c + D_c u_c \quad (40)$$

where x_c is the n_c -dimensional state vector, (A_c, B_c, C_c, D_c) is a minimal realization of $\mathcal{K}(s)$, and $u_c = y_p$.

Define

$$\dot{v} = y_c \quad (41)$$

$$x_z = (x_c^T, v^T)^T \quad (42)$$

$$y_z = v \quad (43)$$

Equations (39)–(43) can be combined as

$$\dot{x}_z = A_z x_z + B_z u_c \quad (44)$$

$$y_z = C_z x_z \quad (45)$$

where

$$A_z = \begin{bmatrix} A_c & 0 \\ C_c & 0 \end{bmatrix} \quad B_z = \begin{bmatrix} B_c \\ D_c \end{bmatrix} \quad C_z = [0 \quad I_k] \quad (46)$$

The closed-loop system is shown in figure 3. The nonlinear plant is stabilized by $\mathcal{K}(s)$ if the closed-loop system (with $\mathcal{K}(s)$ represented by its minimal realization) is globally asymptotically stable.

Theorem 4: Consider the nonlinear plant in equation (21) with y_p as the output. Suppose that

1. The matrix A_c is strictly Hurwitz
2. An $(n_c + k) \times (n_c + k)$ matrix $P_z = P_z^T > 0$ exists such that

$$A_z^T P_z + P_z A_z = -Q_z \equiv -\text{diag}\left(L_c^T L_c, 0_k\right) \quad (47)$$

where L_c is the $k \times n_c$ matrix such that (L_c, A_c) is observable, and $L_c(sI - A_c)^{-1}B_c$ has no transmission zeros in $\text{Re}[s] \geq 0$

$$3. \quad C_z = B_z^T P_z \quad (48)$$

4. The controller $\mathcal{K}(s) = C_c(sI - A_c)^{-1}B_c + D_c$ has no transmission zeros at the origin

Then $\mathcal{K}(s)$ stabilizes the nonlinear plant.

Proof: First consider the system shown in figure 4(a). The nonlinear plant is given by equation (2), and its state vector is taken to be $(q^T, \dot{p}^T)^T$ (i.e., $(\gamma^T, \theta^T)^T$ is not included in the state vector). Now consider the Lyapunov function

$$V = \frac{1}{2}\dot{p}^T M(p)\dot{p} + \frac{1}{2}q^T \tilde{K}q + \frac{1}{2}x_z^T P_z x_z \quad (49)$$

where \tilde{K} is the symmetric positive-definite part of K (i.e., the part associated with nonzero stiffness). Note that V is positive-definite in the state vector $(q^T, \dot{p}^T)^T$ because the mass-inertia matrix $M(p)$, as stated previously, is symmetric positive-definite and uniformly bounded from below and above. Then

$$\dot{V} = \dot{p}^T M(p)\ddot{p} + \frac{1}{2}\dot{p}^T \dot{M}\dot{p} + \dot{q}^T \tilde{K}q + \frac{1}{2}\left(\dot{x}_z^T P_z x_z + x_z^T P_z \dot{x}_z\right) \quad (50)$$

After substitution for $M(p)\ddot{p}$ from equation (2) and for \dot{x}_z from equation (44), equation (50) becomes

$$\begin{aligned} \dot{V} = & \dot{p}^T B^T u - \dot{q}^T \tilde{D}\dot{q} + \dot{p}^T \left(\frac{1}{2}\dot{M} - C \right) \dot{p} - \dot{p}^T K p + \dot{q}^T \tilde{K} q \\ & + \frac{1}{2} \left[\left(x_z^T A_z^T + u_c^T B_z^T \right) P_z x_z + x_z^T P_z (A_z x_z + B_z u_c) \right] \end{aligned} \quad (51)$$

Property \mathcal{S} of the system makes the matrix $(\frac{1}{2}\dot{M} - C)$ *skew-symmetric*, and

$$\dot{V} = \dot{p}^T B^T u - \dot{q}^T \tilde{D}\dot{q} + \frac{1}{2}x_z^T (A_z^T P_z + P_z A_z) x_z + \frac{1}{2}u_c^T (B_z^T P_z) x_z + \frac{1}{2}x_z^T (P_z B_z) u_c \quad (52)$$

$$\dot{V} = -\dot{q}^T \tilde{D}\dot{q} + \dot{p}^T B^T u - \frac{1}{2}x_z^T Q_z x_z + x_z^T C_z^T u_c \quad (53)$$

where equations (47) and (48) have been used. Noting that $u = -y_z = -C_z x_z$ and $B\dot{p} = y_r = u_c$ (fig. 4(a)),

$$\dot{V} = -\dot{q}^T \tilde{D}\dot{q} - \frac{1}{2}x_z^T Q_z x_z - u_c^T y_z + y_z^T u_c \quad (54)$$

from which

$$\dot{V} = -\dot{q}^T \tilde{D}\dot{q} - \frac{1}{2}x_z^T Q_z x_z \quad (55)$$

Because \tilde{D} is positive-definite, $\dot{V} \leq 0$ (i.e., \dot{V} is negative-semidefinite) and the system is Lyapunov-stable. Now, $\dot{V} = 0$ only if $\dot{q} = 0$ and $L_c x_c = 0$. Therefore, either $y_r = 0$ or y_r consists only of terms such as $\nu t^l e^{z_0 t}$ where ν is a constant vector and z_0 is a transmission zero of (A_c, B_c, L_c) . No transmission zeros of (A_c, B_c, L_c) exist in $\text{Re}(s) \geq 0$, which requires that $y_r \rightarrow 0$ exponentially. Because (A_c, B_c, L_c) is minimal and stable, $x_c \rightarrow 0$ exponentially. But, $y_r \rightarrow 0 \Rightarrow \dot{\theta} \rightarrow 0$ and $\omega \rightarrow 0 \Rightarrow \dot{p} \rightarrow 0$; this then implies that $\ddot{p} \rightarrow 0$. By substitution in equation (2), $\gamma \rightarrow \gamma_{ss}$, $\theta \rightarrow \theta_{ss}$, $q \rightarrow 0$, and $u \rightarrow 0$, where γ_{ss} and θ_{ss} are some steady-state values of γ and θ , respectively.

Now consider the configuration shown in figure 4(b), which is realized by application of the following similarity transformation to the system in equation (44):

$$\hat{T} = \begin{bmatrix} I_k & 0 & 0 \\ 0 & A_c & B_c \\ 0 & C_c & D_c \end{bmatrix} \quad (56)$$

Clearly, \hat{T} is nonsingular if and only if $\mathcal{K}(s)$ has no transmission zeros at the origin. The transformed system has controller state equations

$$\dot{x}_c = A_c x_c + B_c y_p \quad (57)$$

$$u = -y_z = -(C_c x_c + D_c y_p) \quad (58)$$

where $y_p = (\gamma^T, \theta^T)^T$. Because transformation \hat{T} is nonsingular, the transformed system is also Lyapunov-stable. The system will now be shown to be, in fact, g.a.s.

Refer to figure 4(b) and see that the output y_p tends to some steady-state value $\bar{y}_p = (\gamma_{ss}^T, \theta_{ss}^T)^T$. Because $\mathcal{K}(s)$ has no zeros at the origin and is stable, its output $y_z = -u$ will also tend to some steady-state \bar{y}_z . Consequently, if $\bar{y}_p \neq 0$, the control input u will tend to a constant value $\bar{u} \neq 0$. However, this contradicts the previously proven fact that $u \rightarrow 0$. Therefore, $y_p \rightarrow 0$ and $x_c \rightarrow 0$ because $\mathcal{K}(s)$ is stable. From LaSalle's invariance theorem this proves that the system is asymptotically stable. Because V is radially unbounded, the system is g.a.s. Q.E.D.

Because no assumptions were made with regard to the model order as well as to the knowledge of the parametric values, the stability is robust to modeling errors and parametric uncertainties.

Remark 1: In theorem 4, if equation (47) holds with a positive-definite matrix Q_c replacing $L_c^T L_c$, then the closed-loop system is g.a.s. In this case the observability and minimum phase property of condition 2 are not needed.

Remark 2: The controller $\mathcal{K}(s)$ stabilizes the complete plant; i.e., the system consisting of the rigid modes, the elastic modes, and the compensator state vector x_c is g.a.s. The global asymptotic stability is guaranteed regardless of the number of modes in the model or parameter uncertainties. The order of the controller can be chosen to be any number $\geq k$. In other words, these results enable the design of a controller of essentially any desired order, which robustly stabilizes the plant. A procedure for designing \mathcal{K} is to choose $Q_z = \text{diag}(Q_c, 0_k)$ where $Q_c = Q_c^T > 0$ and to choose a stable A_c and matrices B_c and C_c so that equations (47) and (48) are satisfied. Using equations (46) and defining

$$P_z = \begin{bmatrix} P_{z1} & P_{z2} \\ P_{z2}^T & P_{z3} \end{bmatrix}$$

where P_{z1} is $n_c \times n_c$ and P_{z3} is $k \times k$, conditions 2 and 3 of theorem 4 can be expanded as

$$\left. \begin{aligned} P_{z1}A_c + A_c^T P_{z1} + P_{z2}C_c + C_c^T P_{z2}^T &= -Q_c \\ P_{z2}^T A_c + P_{z3}C_c &= 0 \\ B_c^T P_{z1} + D_c^T P_{z2}^T &= 0 \\ B_c^T P_{z2} + D_c^T P_{z3} &= I \end{aligned} \right\} \quad (59)$$

In addition, P_z must be positive-definite. Because of the large number of free parameters (A_c, B_c, C_c, D_c, Q_c), the use of equations (59) to obtain the compensator is generally not straightforward. Another method is to use the s -domain equivalent of theorem 4. Theorem 5 gives these equivalent conditions on \mathcal{K} in the s -domain.

Theorem 5: The closed-loop system given by equations (21), (57), and (58) is g.a.s. if $\mathcal{K}(s)$ has no transmission zeros at $s = 0$, and $\mathcal{K}(s)/s$ is MSPR.

Proof: The proof can be obtained by a slight modification of the results of reference 29 to show that the theorem statement implies the conditions of theorem 4.

The condition that $\mathcal{K}(s)/s$ be MSPR is sometimes much easier to check than the conditions of theorem 1. For example, let $\mathcal{K}(s) = \text{diag}[\mathcal{K}_1(s), \dots, \mathcal{K}_k(s)]$, where

$$\mathcal{K}_i(s) = k_i \frac{s^2 + \beta_{1i}s + \beta_{0i}}{s^2 + \alpha_{1i}s + \alpha_{0i}} \quad (60)$$

A straightforward analysis shows that $\mathcal{K}(s)/s$ is MSPR if, and only if, k_i , α_{0i} , α_{1i} , β_{0i} , and β_{1i} are positive for $i = 1, 2, \dots, k$, and

$$\alpha_{1i} - \beta_{1i} > 0 \quad (61)$$

$$\alpha_{1i}\beta_{0i} - \alpha_{0i}\beta_{1i} > 0 \quad (62)$$

For higher order \mathcal{K}_i 's, the conditions on the polynomial coefficients are harder to obtain. One systematic procedure for obtaining such conditions for higher order controllers is the application of Sturm's theorem. (See ref. 27.) Symbolic manipulation codes can then be used to derive explicit inequalities. The controller design problem can be subsequently posed as a constrained optimization problem which minimizes a given performance function. However, the case of fully populated $\mathcal{K}(s)$ has no straightforward method of solution and remains an area for future research.

The following results, which address the cases with static dissipative controllers when the actuators have first- and second-order dynamics, are an immediate consequence of theorem 5 and are stated without proof.

Corollary 5.1: For the static dissipative controller (eq. (22)), suppose that G_p and G_r are diagonal with positive entries denoted by subscript i , and actuators represented by the transfer function $G_{Ai}(s) = k_i/(s + a_i)$ are present in the i th control channel. Then the closed-loop system is g.a.s. if $G_{ri} > G_{pi}/a_i$ (for $i = 1, 2, \dots, k$).

Corollary 5.2: Suppose that the static dissipative controller also includes the feedback of the acceleration y_a , that is,

$$u = -G_p y_p - G_r y_r - G_a y_a$$

where G_p , G_r , and G_a are diagonal with positive entries. Suppose that the actuator dynamics for the i th input channel are given by $G_{Ai}(s) = k_i/(s^2 + \mu_i s + \nu_i)$ with k_i , μ_i , and ν_i positive. Then the closed-loop system is a.s. if

$$\frac{G_{ri}}{G_{ai}} \leq \mu_i < \frac{G_{ri}}{G_{pi}} \quad (i = 1, 2, \dots, k)$$

5.3.3. Realization of \mathcal{K} as strictly proper controller. The controller $\mathcal{K}(s)$ (eqs. (57) and (58)) is not strictly proper because of the direct transmission term D_c . From a practical viewpoint, a strictly proper controller is sometimes desirable because it attenuates sensor noise as well as high-frequency disturbances. Furthermore, the most common types of controllers, which include the linear quadratic Gaussian (LQG) controllers as well as the observer-pole placement controllers, are strictly proper; they have a first-order rolloff. In addition, the realization in equations (57) and (58) does not utilize the rate measurement y_r . The following result states that \mathcal{K} can be realized as a strictly proper controller wherein both y_p and y_r are utilized.

Theorem 6: The nonlinear plant with y_p and y_r as outputs is stabilized by the n_c -dimensional controller \mathcal{K}' given by

$$\dot{\bar{x}}_c = A_c \bar{x}_c + [B_c - A_c L \quad L] \begin{bmatrix} y_p \\ y_r \end{bmatrix} \quad (63)$$

$$y_c = C_c \bar{x}_c \quad (64)$$

where C_c is assumed to be of full rank, and an $n_c \times k$ ($n_c \geq k$) matrix L is a solution of

$$D_c - C_c L = 0 \quad (65)$$

Proof: Consider the controller realization equations (57) and (58). Let

$$\bar{x}_c = x_c + L y_p \quad (66)$$

where L is an $n_c \times k$ matrix. The differentiation of equation (66), use of equations (57) and (58), and replacement of \dot{y}_p with y_r results in equation (63) and leads to

$$y_c = C_c \bar{x}_c + (D_c - C_c L) y_p \quad (67)$$

If L is chosen to satisfy equation (65), the strictly proper controller is given by equations (63) and (64). Equation (65) represents k^2 equations in kn_c unknowns. If $k < n_c$ (i.e., the compensator order is greater than the number of plant inputs) and C_c is of full rank, many possible solutions exist for L . The solution which minimizes the Frobenius norm of L is

$$L = C_c^T (C_c C_c^T)^{-1} D_c \quad (68)$$

If $k = n_c$, equation (68) gives the unique solution $L = C_c^{-1} D_c$.

6. Linear Single-Body Spacecraft

In this section, the case of a single-body flexible spacecraft is considered, which is a special case of the systems discussed in section 5. The motivation for investigating this case separately is that a number of spacecraft belong to this class (e.g., flexible space antennas). In addition, the mathematical models for this class of spacecraft are linear, which permits the use of a variety of

controller synthesis techniques that are not available for nonlinear systems. However, the basic stability results for the linear case under static and dynamic dissipative compensation can be obtained as special cases of the stability results for nonlinear models. (Refer to section 5.)

6.1. Linearized Mathematical Model

The linearized mathematical model of the rotational dynamics of single-body flexible space structure can be obtained by linearizing equation (2) about the zero steady state and is given by

$$\widehat{M}\ddot{p} + \widehat{K}p = B^T u \quad (69)$$

where

$$p = \begin{pmatrix} \eta^T, q^T \end{pmatrix}^T \quad \eta = (\phi, \theta, \psi)^T \quad (70)$$

Here, η represents the 3×1 attitude vector, q is the $n_q \times 1$ vector of elastic modal amplitudes ($n_q = n - 3$), \widehat{M} is the positive-definite symmetric mass-inertia matrix (note that \widehat{M} is constant in this case), \widehat{K} is the positive-semidefinite stiffness matrix related to the flexible degrees of freedom, u is the 3×1 input torque vector, and $B = [I_3, 0_{3 \times n_q}]$. The system in equation (69) can be transformed into modal form by using transformation $\zeta = \Phi p$, where Φ is the eigenvector matrix such that $\Phi^T \widehat{M} \Phi = I$ and $\phi^T \widehat{K} \Phi = \widetilde{C}$, a diagonal matrix. The resulting model is

$$\ddot{\zeta} + \widetilde{C}\zeta = \Phi^T B^T u = \begin{bmatrix} \overline{\Phi}_{11}^T \\ \overline{\Phi}_{12}^T \end{bmatrix} u \quad (71)$$

where $\overline{\Phi}_{11}^T$ and $\overline{\Phi}_{12}^T$ are 3×3 and $n_q \times 3$ matrices, respectively, and matrix \widetilde{C} is given by

$$\widetilde{C} = \text{diag}(0_3, \Lambda) \quad (72)$$

where

$$\Lambda = \text{diag}(\omega_1^2, \omega_2^2, \dots, \omega_{n_q}^2) \quad (73)$$

in which ω_i ($i = 1, 2, \dots, n_q$) represent the elastic mode frequencies. The first three components of ζ correspond to rigid-body modes. The rigid-body modes are controllable if, and only if, $\overline{\Phi}_{11}$ is nonsingular. Because one torque actuator is used for each of the X -, Y -, and Z -axes, $\overline{\Phi}_{11}$ is nonsingular. Note that the mass-inertia matrix in this modal form is the 3×3 identity matrix. However, the model is customarily used in a slightly modified form wherein the elastic motion is superimposed on the rigid-body motion. (See ref. 4.) This can be achieved as follows. Suppose $J = J^T > 0$ is the moment-of-inertia matrix of the spacecraft. Then, with the use of the transformation, $\zeta = \Delta \xi$ where the transformation matrix Δ is given by

$$\Delta = \begin{bmatrix} \overline{\Phi}_{11}^T J & 0_{3 \times n_q} \\ 0_{n_q \times 3} & I_{n_q \times n_q} \end{bmatrix} \quad (74)$$

Equation (71) is transformed to

$$\Delta \ddot{\xi} + \widetilde{C} \Delta \xi = \begin{bmatrix} \overline{\Phi}_{11}^T \\ \overline{\Phi}_{12}^T \end{bmatrix} u \quad (75)$$

Premultiplication of the above equation by Δ^{-1} yields

$$\ddot{\xi} + \Delta^{-1} \widetilde{C} \Delta \xi = \begin{bmatrix} J^{-1} \\ \overline{\Phi}_{12}^T \end{bmatrix} u \quad (76)$$

Note that $\Delta^{-1}\tilde{C}\Delta = \tilde{C}$ and with premultiplication by $\text{diag}(J, I_{n_q})$, equation (76) can be rewritten as

$$\tilde{A}\ddot{z} + \tilde{C}z = \Gamma^T u \quad (77)$$

where $\tilde{A} = \text{diag}(J, I)$ and $\Gamma = [I_3, \bar{\Phi}_{12}]$. The inherent structural damping term \tilde{B} can now be added to give the design model as follows:

$$\tilde{A}\ddot{\xi} + \tilde{B}\dot{\xi} + \tilde{C}\xi = \Gamma^T u \quad (78)$$

where

$$\tilde{A} = \text{diag}(J, I_{n_q}) \quad (79)$$

$$\tilde{B} = \text{diag}(0_3, D) \quad (80)$$

$$\tilde{C} = \text{diag}(0_3, \Lambda) \quad (81)$$

$$\Lambda = \text{diag}(\omega_1^2, \omega_2^2, \dots, \omega_{n_q}^2) \quad (82)$$

(eqs. (81) and (82) are the same as eqs. (72) and (73), respectively), $D = D^T > 0$ is the $n_q \times n_q$ matrix representing the inherent damping in the elastic modes, ω_i ($i = 1, 2, \dots, n_q$) represents the elastic mode frequencies, and

$$\Gamma = [I_{3 \times 3} \quad \bar{\Phi}_{12}] \quad (83)$$

The attitude and attitude rate sensor outputs are given by

$$y_p = \Gamma z \quad (84)$$

$$y_r = \Gamma \dot{z} \quad (85)$$

where y_p and y_r are 3×1 measured position and rate vectors, respectively.

All of the stability results of section 5 for static and dynamic dissipative controllers are directly applicable to this case. From theorem 2, the constant gain dissipative control law is given by

$$u = -G_p y_p - G_r y_r \quad (86)$$

where G_p and G_r , which are symmetric, positive-definite, proportional and rate gain matrices, respectively, make the closed-loop system asymptotically stable. Furthermore from theorem 3, the stability is robust in the presence of monotonically nondecreasing actuator nonlinearities and sensor nonlinearities belonging to the $(0, \infty)$ sector.

For this case, note that the transfer function is given by $G(s) = G'(s)/s$ (fig. 5), where $G'(s)$ is given by

$$G'(s) = \frac{J^{-1}}{s} + \sum \frac{\Phi_i \Phi_i^T s}{s^2 + 2\rho_i \omega_i s + \omega_i^2} \quad (87)$$

where J is the moment-of-inertia matrix, and Φ_i , ρ_i , and ω_i denote the rotational mode shape matrix, damping ratio, and natural frequency, respectively, of the i th structural mode. The operator represented by the transfer function $G'(s)$ is passive. Because this operator is linear and time-invariant, its passivity implies that the transfer function $G'(s)$ is positive-real. However, the transfer function $G(s)$, from u to y_p , is not positive-real. This system is robustly stabilized by dynamic dissipative compensator $\mathcal{K}(s)$ satisfying the conditions of theorems 4 and 5. The compensator can be realized as a strictly proper one as shown in theorem 6.

6.2. Optimal Dynamic Dissipative Compensator

The results of theorems 5 and 6 can be applied to check if a given model-based controller, such as an LQG controller, is dissipative (i.e., if it robustly stabilizes $G(s)$). In particular, the following result is obtained.

Theorem 7: Consider the n_k th-order LQG controller given by

$$\dot{\varsigma} = A_{\varsigma}\varsigma + H \begin{bmatrix} y_p \\ y_r \end{bmatrix} \quad (88)$$

$$u = F\varsigma \quad (89)$$

where A_{ς} is the closed-loop LQG compensator matrix

$$A_{\varsigma} = A_0 - B_0F + HC_0 \quad (90)$$

A_0 , B_0 , and C_0 denote the design model matrices, and F and H are the regulator and estimator gain matrices, respectively. This controller robustly stabilizes the system if the rational matrix $M(s)/s$ is MSPR where

$$M(s) = F(sI - A_{\varsigma})^{-1}(H_1 + A_{\varsigma}H_2) + FH_2 \quad (91)$$

and H_1 and H_2 denote the matrices consisting of the first three columns and the last three columns of H , respectively.

The theorem can be proved by using the transformation $\hat{x} = \varsigma - H_2y_p$ in equation (88). Although a given LQG controller will not be likely to satisfy the condition of theorem 7, the condition can be incorporated as a constraint in the design process. The problem can be posed as one of minimizing a given LQG performance function with the constraint that $M(s)/s$ is MSPR. Also note that theorem 7 is not limited to an LQG controller but is valid for any observer-based controller with control gain F and observer gain H . Another way of posing the design problem is to obtain the dissipative compensator which is closest to a given LQG design. The distance between compensators can be defined as either

1. The distance between the compensator transfer functions in terms of H_2 or H_{∞} norm of the difference or
2. The distance between the matrices used in the realization in terms of a matrix (i.e., spectral or Frobenius) norm

For example, the dissipative compensator A_c and C_c matrices can be taken to be the LQG A_{ς} and F matrices, respectively, and the compensator B_c and D_c matrices can be chosen to minimize δ as follows while still satisfying the MSPR constraint:

$$\delta = \left\| \begin{bmatrix} B_c - (H_1 + A_{\varsigma}H_2) \\ D_c - FH_2 \end{bmatrix} \right\|_{2 \text{ or } \infty} \quad (92)$$

Thus the design method usually ends up as a constrained optimization problem.

7. Numerical Examples

Two numerical examples are given to demonstrate some of the results obtained in sections 4 and 6. The first example consists of a conceptual nonlinear model of a spacecraft with two flexible articulated appendages. The stability results for the nonlinear dissipative control law given in

section 4 are verified by simulation. The second example addresses attitude control system design for a large space antenna, which is modeled as a linear single-body structure. The objective of the control system is to minimize a prescribed quadratic performance index. For this system, the conventional LQG controller design was found to have stability problems due to unmodeled high-frequency dynamics and parametric uncertainties. However, the dynamic dissipative controller designed to minimize the quadratic performance function resulted in good performance with guaranteed stability in the presence of both unmodeled dynamics and parametric uncertainties.

7.1. Two-Link Flexible Space Robot

The system shown in figure 6 is used for validation of the theoretical results obtained in section 4. The configuration consists of a central body with two articulated flexible links attached to it and resembles a flexible space robot. The central body is a solid cylinder 1.0 m in diameter and 2 m in height. Each link is modeled in MSC/NASTRAN¹ as a 3-m-long flexible beam with 20 bar elements. The circular cross sections of the links are 1.0 cm in diameter resulting in significant flexibility. The material chosen for the central body as well as the links has a mass density of 2.568×10^{-3} kg/m³ and modulus of elasticity $E = 6.34 \times 10^9$ kg/m². The central-body mass is 4030 kg and each link mass is 0.605 kg. The principal moments of inertia of the central-body about local X -, Y -, and Z -axes are 1600, 1600, and 500 kg-m², respectively. Each link can rotate about its local Z -axis. The link moment of inertia about its axis of rotation is 1.815 kg-m². The central body has three rotational degrees of freedom. As shown in figure 6, two revolute joints exist: one between the central-body and link 1 and another between links 1 and 2. The axes of rotation for revolute joints 1 and 2 coincide with the local Z -axes of links 1 and 2, respectively. Collocated actuators and sensors are assumed for each rigid degree of freedom. Sensor measurements are also assumed to be available for the central-body attitude (quaternions) and rates as well as revolute joint angles and rates.

The first link was modeled as a flexible beam with pinned-pinned boundary conditions; the second link was modeled as a flexible beam with pinned-free boundary conditions. For the purpose of simulation, the first four bending modes in the local XY -plane were considered for each link (i.e., the system has five rigid rotational degrees of freedom and eight flexible degrees of freedom, four for each link). The modal data were obtained from MSC/NASTRAN. The mode shapes and the frequencies for links 1 and 2 are shown in figures 7 and 8, respectively. A complete nonlinear simulation was obtained with DADS², a commercially available software.

A rest-to-rest maneuver was considered to demonstrate the control law. The initial configuration was equivalent to $(\pi/4)$ -rad rotation of the entire spacecraft about the global X -axis and 0.5-rad rotation of the revolute joint 2. The objective of the control law was to restore the zero state of the system. A nonlinear dissipative controller (eq. (13)) was used to accomplish the task. Because there are no known techniques to date for the synthesis of such controllers, the selection of controller gains was based on trial and error. Based on several trials, the following gains were found to give the desirable response: $G_{p1} = \text{diag}(500, 500, 500)$, $G_{p2} = \text{diag}(50, 50)$, and $G_r = \text{diag}(500, 275, 270, 100, 100)$. As the system begins motion, all members move relative to one another, and dynamic interaction exists between members. Complete nonlinear and coupling effects are incorporated in the simulation. The Euler parameter responses are shown in figures 9 and 10, and the joint angle displacements for the revolute joints 1 and 2 are shown in figure 11. The joint displacements decay asymptotically and are nearly zero within 15 sec. The tip displacements with respect to global X -, Y -, and Z -axes are shown in figures 12 and 13. Note that the manipulator tip reaches its desired x position in about 15 sec, whereas the desired y and z positions are reached in about 35 sec. These responses effectively demonstrate the stability

¹ Trademark of The MacNeal-Schwendler Corp., Los Angeles, CA 90041.

² Trademark of Computer Aided Design Software, Inc., Oakdale, IA 52319.

results of section 4. The time histories of control torques are given in figures 14–17. The effects of nonlinearities in the model can be seen in the responses as well as in the torque profiles.

7.2. Application to Hoop-Column Antenna

The 122-m-diameter, hoop-column antenna concept (fig. 18), as described in reference 4, consists of a deployable mast attached to a deployable hoop by cables held in tension. The antenna has many significant elastic modes, which include mast bending, torsion, and reflective surface distortion. The objective is to control the attitude (including rigid and elastic components) at a certain point on the mast in the presence of actuator noise and attitude and rate sensor noise; one attitude and one rate sensor is collocated with a torque actuator for each of the three axes. The open-loop damping ratio is assumed to be 1 percent. A linear quadratic Gaussian (LQG) controller, based on a design model consisting of the three rotational rigid modes and the first three elastic modes, was first designed to minimize

$$\mathcal{J} = \lim_{T \rightarrow \infty} \frac{1}{T} \mathcal{E} \int_0^T \left(y_p^T Q_p y_p + y_r^T Q_r y_r + u^T R u \right) dt \quad (93)$$

with $Q_p = 4 \times 10^8 I_3$, $Q_r = 10^8 I_3$, and $R = \text{diag}(0.1, 0.1, 1)$. The actuator noise covariance intensity was $0.1 I_3$ ft-lb and the attitude and rate sensor noise covariance intensity was $10^{-10} \text{diag}(0.25, 0.25, 2.5)$ rad/sec and $10^{-10} \text{diag}(0.25, 0.25, 2.5)$ rad²/sec², respectively. The optimal value of \mathcal{J} was 0.6036, and the closed-loop eigenvalues for the design model and the 12th-order controller are given in table I.

A dynamic dissipative controller, which consisted of three second-order blocks as in equation (60), was designed next. By using the transformation of theorem 6 with $L = (\gamma_i, \delta_i)^T$ for $\mathcal{K}_i(s)$, each $\mathcal{K}_i(s)$ can be realized as a strictly proper controller

$$\dot{\bar{x}}_{ki} = \begin{bmatrix} 0 & 1 \\ -\alpha_{0i} & -\alpha_{1i} \end{bmatrix} \bar{x}_{ki} + \begin{bmatrix} \delta_i & \gamma_i \\ \beta_{0i}\gamma_i + \beta_{1i}\delta_i & \delta_i \end{bmatrix} \begin{bmatrix} y_{pi} + w_{pi} \\ y_{ri} + w_{ri} \end{bmatrix} \quad (94)$$

$$u = (u_1, u_2, u_3)^T \quad u_i = (\beta_{0i}, -\alpha_{0i}) \bar{x}_{ki} \quad (95)$$

The constraints to be satisfied are equation (61), equation (62), and that α_{0i} , α_{1i} , β_{0i} , and β_{1i} be positive ($i = 1, 2, 3$). Thus, this sixth-order compensator has 18 design variables. The performance function in equation (93) can be computed by solving the steady-state covariance equation for the closed-loop state equation for the plant and the controller. A dynamic dissipative controller (DDC) was designed by performing numerical minimization of the performance function \mathcal{J} with respect to the 18 design variables. To ensure a reasonable transient response, an additional constraint that the real parts of the closed-loop eigenvalues be ≤ -0.0035 is imposed. Table II lists the resulting closed-loop eigenvalues. Although the value of \mathcal{J} for the DDC was 1.2674 (about twice that for the LQG controller), the closed-loop eigenvalues indicate satisfactory damping ratios and decay rates. Furthermore, the LQG controller, which was based on the first six modes, caused instability when higher modes were included in the evaluation model, whereas the DDC yields guaranteed stability in the presence of higher modes as well as parametric uncertainties.

8. Concluding Remarks

Stabilization of a class of nonlinear multibody flexible space systems was considered using a class of dissipative control laws. Robust global asymptotic stability can be obtained with nonlinear feedback of the central-body quaternion angles, relative body angles, and angular velocities. For an important special case wherein the central-body motion is in the linear range

while all the appendages undergo unlimited motion, global asymptotic stability under a linear dissipative control law was proved. Furthermore, the robust stability was showed to be preserved in the presence of a broad class of actuator and sensor nonlinearities and a class of actuator dynamics.

A class of dynamic dissipative controllers was introduced and was proved to provide global asymptotic stability for the case where the central-body motion is small. Dynamic dissipative controllers offer more design freedom than static dissipative controllers and, therefore, can achieve better performance and noise attenuation.

Linear single-body spacecraft represent a special case of nonlinear multibody spacecraft, and therefore, the robust stability results are directly applicable to this case.

All the stability results presented are valid in spite of unmodeled modes and parametric uncertainties; i.e., the stability is robust to model errors. The results have a significant practical value because the mathematical models of such systems usually have substantial inaccuracies, and the actuation and sensing devices have nonlinearities.

Design of dissipative controllers to obtain optimal performance is, as yet, an unsolved problem, especially for the nonlinear case. Future work should address the development of systematic methods for the synthesis of both nonlinear and linear, static and dynamic, dissipative controllers.

NASA Langley Research Center
Hampton, VA 23681-0001
December 23, 1994

Appendix

Mathematical Model Derivation and System Properties

The steps involved in the derivation of equations of motion (eq. (2)) are outlined in this appendix. The details of the derivation of the mass-inertia matrix $M(p)$ and the stiffness matrix \tilde{K} are not included but can be found in reference 14.

Kinetic Energy

The kinetic energy of the system represented in figure 1 is given by

$$T = \frac{1}{2} \dot{p}^T M(p) \dot{p} \quad (\text{A1})$$

where $M(p)$ is the configuration-dependent symmetric and positive-definite mass-inertia matrix of the system and p is the vector of the generalized coordinates.

Potential Energy

Generally, the potential energy of a system has many sources (e.g., elastic displacement or thermal deformation). The deformations due to thermal effects are not considered in the formulation in this paper; however, they can easily be included in the formulation if desired. Thus, the potential energy is assumed to consist of the contribution only from the strain energy due to elastic deformation. Also, the materials under consideration are assumed to be isotropic in nature and to obey Hooke's law.

If \tilde{K} is the stiffness matrix of the system, then the potential energy of the system is given by

$$V = \frac{1}{2} q^T \tilde{K} q$$

where q is the vector of the flexible degrees of freedom. If the matrix K is defined as

$$K = \begin{bmatrix} 0_{k \times k} & 0_{k \times (n-k)} \\ 0_{(n-k) \times k} & \tilde{K}_{(n-k) \times (n-k)} \end{bmatrix}$$

then the potential energy of the system can be rewritten in terms of the generalized variable p as

$$V = \frac{1}{2} p^T K p \quad (\text{A2})$$

Equations of Motion

From equations (A1) and (A2), the Lagrangian of the system is formed as

$$L = T - V$$

For convenience, L can be rewritten in the indicial notation as

$$L = T - V = \frac{1}{2} \sum_{i,j} M_{ij} \dot{p}_i \dot{p}_j - V \quad (\text{A3})$$

The Euler-Lagrange equations for the system can then be derived from

$$\frac{d}{dt} \left(\frac{\partial L}{\partial \dot{p}_k} \right) - \frac{\partial L}{\partial p_k} = F_k \quad (\text{A4})$$

where F_k are generalized forces from the nonconservative force field. From evaluation of the derivatives,

$$\frac{\partial L}{\partial \dot{p}_k} = \sum_j M_{kj} \dot{p}_j \quad (\text{A5})$$

and

$$\begin{aligned} \frac{d}{dt} \left(\frac{\partial L}{\partial \dot{p}_k} \right) &= \sum_j M_{kj} \ddot{p}_j + \sum_j \dot{M}_{kj} \dot{p}_j \\ &= \sum_j M_{kj} \ddot{p}_j + \sum_{i,j} \frac{\partial M_{kj}}{\partial p_i} \dot{p}_i \dot{p}_j \end{aligned} \quad (\text{A6})$$

Also

$$\frac{\partial L}{\partial p_k} = \frac{1}{2} \sum_{i,j} \frac{\partial M_{ij}}{\partial p_k} \dot{p}_i \dot{p}_j - \frac{\partial V}{\partial p_k} \quad (\text{A7})$$

Thus, the Euler-Lagrange equations can be written as

$$\sum_j M_{kj} \ddot{p}_j + \sum_{i,j} \left(\frac{\partial M_{kj}}{\partial p_i} - \frac{1}{2} \frac{\partial M_{ij}}{\partial p_k} \right) \dot{p}_i \dot{p}_j - \frac{\partial V}{\partial p_k} = F_k \quad (k = 1, 2, \dots, n) \quad (\text{A8})$$

By interchanging the order of summation and taking advantage of symmetry,

$$\sum_{i,j} \left(\frac{\partial M_{kj}}{\partial p_i} \right) \dot{p}_i \dot{p}_j = \frac{1}{2} \sum_{i,j} \left(\frac{\partial M_{kj}}{\partial p_i} + \frac{\partial M_{ki}}{\partial p_j} \right) \dot{p}_i \dot{p}_j \quad (\text{A9})$$

Hence,

$$\sum_{i,j} \left(\frac{\partial M_{kj}}{\partial p_i} - \frac{1}{2} \frac{\partial M_{ij}}{\partial p_k} \right) \dot{p}_i \dot{p}_j = \sum_{i,j} \frac{1}{2} \left(\frac{\partial M_{kj}}{\partial p_i} + \frac{\partial M_{ki}}{\partial p_j} - \frac{\partial M_{ij}}{\partial p_k} \right) \dot{p}_i \dot{p}_j \quad (\text{A10})$$

The terms

$$C_{ijk} = \frac{1}{2} \left(\frac{\partial M_{kj}}{\partial p_i} + \frac{\partial M_{ki}}{\partial p_j} - \frac{\partial M_{ij}}{\partial p_k} \right) \quad (\text{A11})$$

are known as Christoffel symbols. For each fixed k , note that $C_{ijk} = C_{jki}$. Also,

$$\frac{\partial V}{\partial p_k} = K_{kj} p_j \quad (\text{A12})$$

Finally, the Euler-Lagrange equations of motion can be written as

$$\sum_j M_{kj} \ddot{p}_j + \sum_{i,j} C_{ijk} \dot{p}_i \dot{p}_j + D_{kj} \dot{p} + K_{kj} p_j = F_k \quad (k = 1, 2, \dots, n) \quad (\text{A13})$$

where D is the inherent structural damping matrix and $D\dot{p}$ is the vector of nonconservative forces.

Of the four terms on the left side of equation (A13), the first term involves second derivatives of the generalized coordinates p . The second term consists of centrifugal terms (e.g., \dot{p}_i^2) and Coriolis terms (e.g., $\dot{p}_i \dot{p}_j$, $i \neq j$). In general, the coefficients C_{ij} are functions of p . The third term involves only the first derivatives of p and corresponds to the dissipative forces due to

inherent damping. The fourth term, which involves only p , arises from the differentiation of the potential energy.

In matrix-vector notation, equation (A13) can be written as

$$M(p)\ddot{p} + C(p, \dot{p})\dot{p} + D\dot{p} + Kp = F \quad (\text{A14})$$

The k, j th element of the matrix $C(p, \dot{p})$ is defined as

$$\begin{aligned} C_{kj} &= \sum_{i=1}^n c_{ijk}(p)\dot{p}_i \\ &= \sum_{i=1}^n \frac{1}{2} \left(\frac{\partial M_{kj}}{\partial p_i} + \frac{\partial M_{ki}}{\partial p_j} - \frac{\partial M_{ij}}{\partial p_k} \right) \dot{p}_i \end{aligned} \quad (\text{A15})$$

An important property of the systems whose equations of motion are given by equation (A14) is derived next. This property is pivotal to the stability results obtained in sections 4 and 5.

Theorem A1: The matrix $S = \dot{M}(p) - 2C(p, \dot{p})$ is skew-symmetric.

Proof: The k, j th element of the time derivative of the mass-inertia matrix $\dot{M}(p)$ is given by the chain rule as

$$\dot{M}_{kj} = \sum_{i=1}^n \frac{\partial M_{kj}}{\partial p_i} \dot{p}_i \quad (\text{A16})$$

Therefore, the k, j th component of $S = \dot{M} - 2C$ is given by

$$\begin{aligned} S_{kj} &= \dot{M}_{kj} - 2C_{kj} \\ &= \sum_{i=1}^n \left[\frac{\partial M_{kj}}{\partial p_i} - \left(\frac{\partial M_{kj}}{\partial p_i} + \frac{\partial M_{ki}}{\partial p_j} - \frac{\partial M_{ij}}{\partial p_k} \right) \right] \dot{p}_i \\ &= \sum_{i=1}^n \left(\frac{\partial M_{ij}}{\partial p_k} - \frac{\partial M_{ki}}{\partial p_j} \right) \dot{p}_i \end{aligned} \quad (\text{A17})$$

Because the inertia matrix is symmetric (i.e., $M_{ij} = M_{ji}$), the interchange of the indices k and j in equation (A17) results in

$$S_{jk} = -S_{kj} \quad (\text{A18})$$

This completes the proof.

Q.E.D.

Theorem A1 can be used to prove that the system given by equations (2) has the important property of passivity as defined in reference 3.

Theorem A2: The input-output map from u to y_r is passive, i.e., with zero initial conditions,

$$\int_0^T y_r^T(t) u(t) dt \geq 0 \quad (\forall T \geq 0) \quad (\text{A19})$$

for all $u(t)$ belonging to the extended Lebesgue space L_{2e}^k .

Proof: Premultiplication of both sides of equations (2) by \dot{p}^T and integration result in

$$\int_0^T \left[\dot{p}^T M(p) \ddot{p} + \dot{p}^T C(p, \dot{p}) \dot{p} + \dot{p}^T D \dot{p} + \dot{p}^T K p \right] dt = \int_0^T y_r^T u dt \quad (\text{A20})$$

Note that

$$\frac{d}{dt} \left[\dot{p}^T M(p) \dot{p} \right] = 2\dot{p}^T M(p) \ddot{p} + \dot{p}^T \dot{M}(p) \dot{p} \quad (\text{A21})$$

Application of theorem A1 and simplification yields

$$\frac{1}{2} \dot{p}^T(T) M[p(T)] \dot{p}(T) + \int_0^T \dot{p}^T D \dot{p} dt + \frac{1}{2} p^T(T) K p(T) = \int_0^T y_r^T u dt \quad (\text{A22})$$

Because the left side of equation (A22) is nonnegative for all $T \geq 0$, this gives the required result.
Q.E.D.

References

1. Asrar, Ghassem; and Dokken, David Jon, eds.: *1993 Earth Observing System Reference Handbook*. NASA NP-202, 1993.
2. General Electric Co.: *Upper Atmosphere Research Satellite (UARS) Project Data Book*. NASA CR-193176, 1987.
3. Desoer, Charles A.; and Vidyasagar, M.: *Feedback Systems: Input-Output Properties*. Academic Press, 1975.
4. Joshi, S. M.: *Control of Large Flexible Space Structures*. Volume 131 of *Lecture Notes in Control and Information Sciences*, M. Thoma and A. Wyner, eds., Springer-Verlag, 1989.
5. Meirovitch, Leonard: *Methods of Analytical Dynamics*. McGraw-Hill Book Co., Inc., 1970.
6. Takegaki, M.; and Arimoto, S.: A New Feedback Method for Dynamic Control of Manipulators. *J. Dyn. Syst., Meas. & Control*, vol. 103, June 1981, pp. 119–125.
7. Koditschek, Dan: Natural Motion for Robot Arms. *Proceedings of the 23rd Conference on Decision and Control*, IEEE, Dec. 1984, pp. 733–735.
8. Spong, Mark W.; and Vidyasagar, M.: *Robot Dynamics and Control*. John Wiley & Sons, Inc., 1989.
9. Vidyasagar, M.: *Nonlinear Systems Analysis*. Prentice-Hall, Inc., 1993.
10. Wen, John T.; and Bayard, David S.: New Class of Control Laws for Robotic Manipulators. *Int. J. Control*, vol. 47, May 1988, I—Nonadaptive Case, pp. 1361–1385, and II—Adaptive Case, pp. 1387–1406.
11. Paden, Brad; and Panja, Ravi: Globally Asymptotically Stable ‘PD+’ Controller for Robot Manipulators. *Int. J. Control*, vol. 47, June 1988, pp. 1697–1712.
12. Paden, Brad; Riedle, Brad; and Bayo, Eduardo: Exponentially Stable Tracking Control for Multi-Joint Flexible-Link Manipulators. *Proceedings of the 9th American Control Conference*, Volume 1, IEEE, 1990, pp. 680–684.
13. Juang, Jer-Nan; Wu, Shih-Chin; Phan, Minh; and Longman, Richard W.: Passive Dynamic Controllers for Nonlinear Mechanical Systems. *J. Guid., Control, & Dyn.*, vol. 16, no. 5, Sept.–Oct. 1993, pp. 845–851.
14. Kelkar, Atul G.: *Mathematical Modeling of a Class of Multibody Flexible Space Structures*. NASA TM-109166, 1994.
15. Greenwood, Donald T.: *Principles of Dynamics*. Prentice-Hall, Inc., 1965.
16. Wen, John Ting-Yung; and Kreutz-Delgado, Kenneth: The Attitude Control Problem. *IEEE Trans. Autom. Control*, vol. 36, Oct. 1991, pp. 1148–1162.
17. Kane, T. R.: Solution of Kinematical Differential Equations for a Rigid Body. *J. Appl. Mech.*, vol. 4, Mar. 1973, pp. 109–113.
18. Ickes, B. P.: A New Method for Performing Digital Control System Attitude Computations Using Quaternions. *AIAA J.*, vol. 8, 1970, pp. 13–17.
19. Harding, C. F.: Solution to Euler’s Gyrodynamics. *J. Appl. Mech.*, vol. 31, June 1964, pp. 325–328.
20. Haug, Edward J.: *Computer Aided Kinematics and Dynamics of Mechanical Systems*. Allyn and Bacon, 1989.
21. Benhabib, R. J.; Iwens, R. P.; and Jackson, R. L.: Stability of Large Space Structure Control Systems Using Positivity Concepts. *J. Guid. & Control*, vol. 4, no. 5, Sept.–Oct. 1981, pp. 487–494.
22. McLaren, M. D.; and Slater, G. L.: Robust Multivariable Control of Large Space Structures Using Positivity. *J. Guid., Control, & Dyn.*, vol. 10, no. 4, July–Aug. 1987, pp. 393–400.
23. Slater, G. L.; and McLaren, M. D.: Estimator Eigenvalue Placement in Positive Real Control. *J. Guid., Control, & Dyn.*, vol. 13, Jan.–Feb. 1990, pp. 168–175.
24. Popov, V. M.: *Hyperstability of Control Systems*. Springer-Verlag, 1973.
25. Lozano-Leal, Rogelio; and Joshi, Suresh M.: Strictly Positive Real Transfer Functions Revisited. *IEEE Trans. Autom. Control*, vol. 35, no. 11, Nov. 1990, pp. 1243–1245.
26. Joshi, S. M.; Maghami, P. G.; and Kelkar, A. G.: Dynamic Dissipative Compensator Design for Large Space Structures. *A Collection of Technical Papers, AIAA Guidance, Navigation and Control Conference*, Volume 1, Aug. 1991, pp. 467–477. (Available as AIAA-91-2650-CP.)

27. Van Valkenburg, M. E.: *Introduction to Modern Network Synthesis*. John Wiley & Sons, Inc., 1960.
28. Anderson, B. D. O.: A System Theory Criterion for Positive Real Matrices. *SIAM J. Control*, vol. 5, no. 2, May 1967, pp. 171–182.
29. Joshi, Suresh M.; and Gupta, Sandeep: *Robust Stabilization of Marginally Stable Positive-Real Systems*. NASA TM-109136, 1994.

Table I. Closed-Loop Eigenvalues for LQG Controller

Regulator	Estimator
$-0.0238 \pm 0.0542i$	$-0.0240 \pm 0.0544i$
$-0.0721 \pm 0.0964i$	$-0.0720 \pm 0.0965i$
$-0.0754 \pm 0.1000i$	$-0.0725 \pm 0.0963i$
$-0.3169 \pm 0.8108i$	$-0.4050 \pm 0.7703i$
$-0.2388 \pm 1.3554i$	$-0.3334 \pm 1.3333i$
$-0.3375 \pm 1.7030i$	$-0.5104 \pm 1.6562i$

Table II. Closed-Loop Eigenvalues for
Dynamic Dissipative Controller

$-0.0035 \pm 0.0194i$
$-0.0183 \pm 0.0458i$
$-0.0160 \pm 0.0502i$
$-0.3419 \pm 0.5913i$
$-0.7179 \pm 0.6428i$
$-0.8479 \pm 0.5653i$
$-0.6482 \pm 1.6451i$
$-0.4536 \pm 2.1473i$
$-0.3764 \pm 2.5522i$

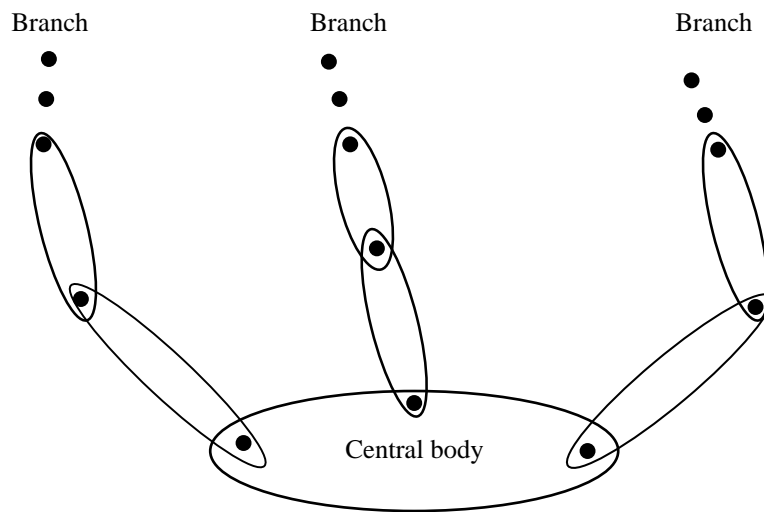
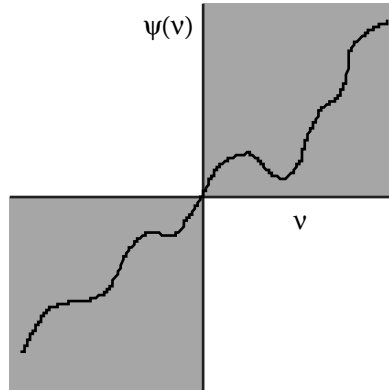
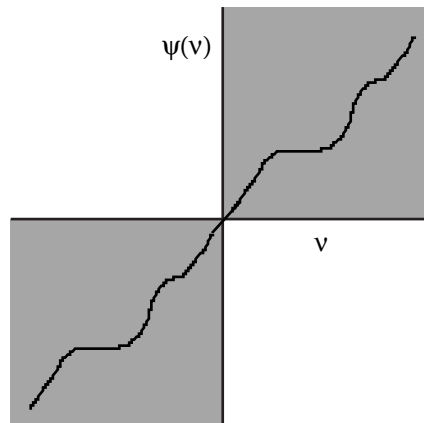


Figure 1. Multibody system.



(a) $(0, \infty)$ -sector nonlinearity.



(b) $(0, \infty)$ -sector monotonically nondecreasing nonlinearity.

Figure 2. Examples of nonlinearities.

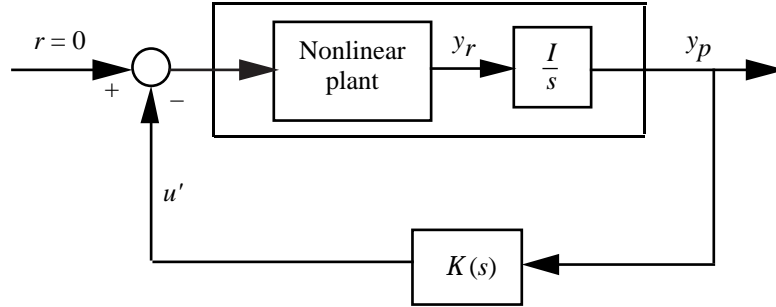
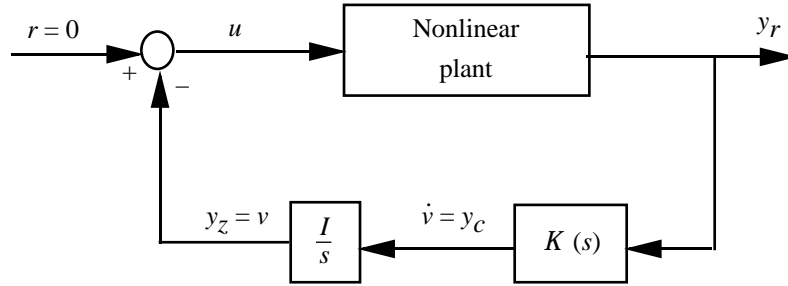
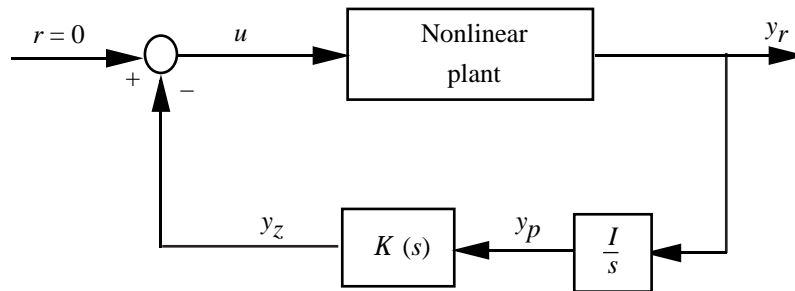


Figure 3. Feedback closed-loop configuration.



(a) Compensator with rate input.



(b) Compensator with position input.

Figure 4. Rearrangement of feedback loops.

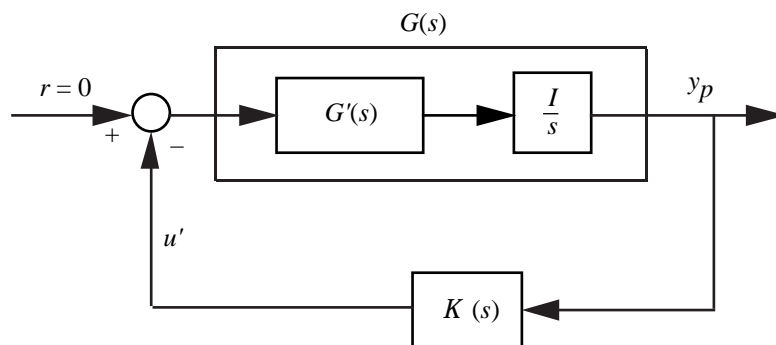


Figure 5. Feedback loop for linear case.

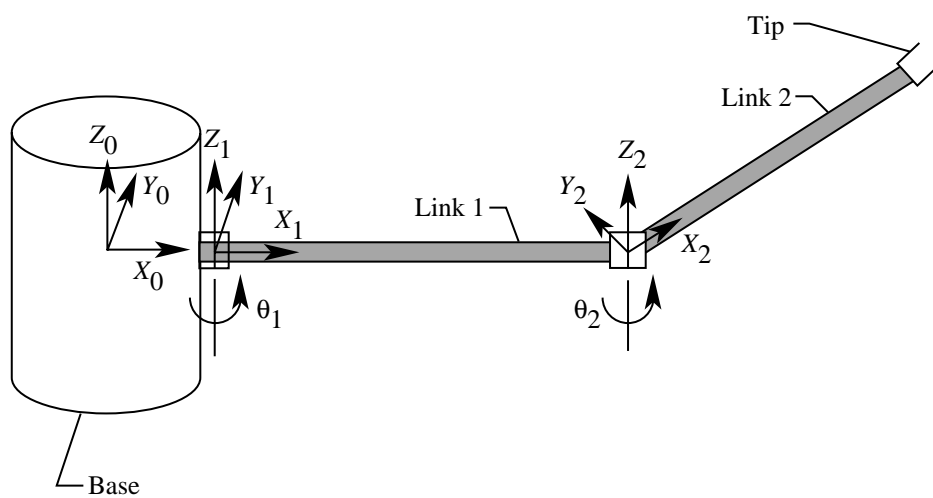
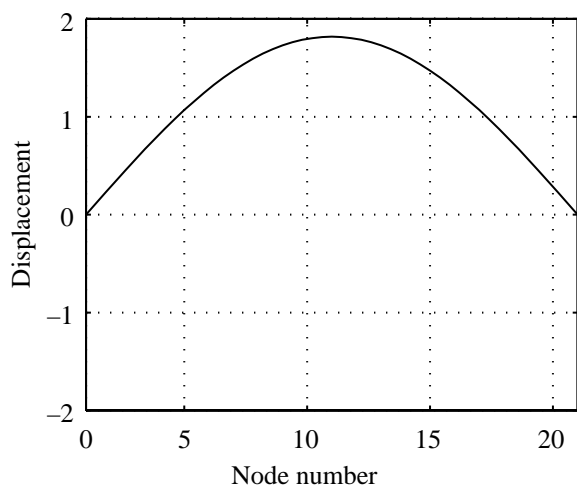
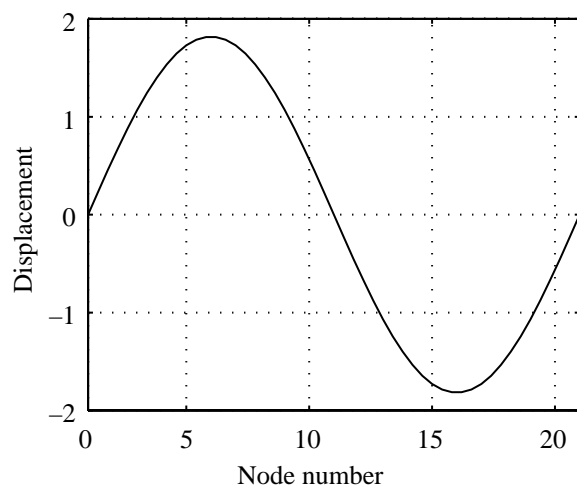


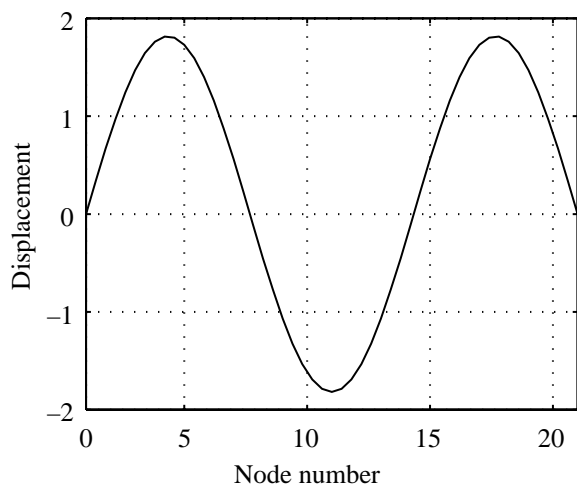
Figure 6. Flexible space robot.



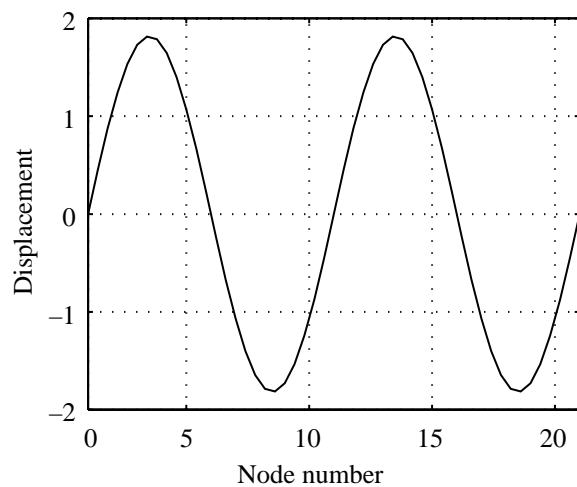
(a) Mode 1; frequency = 2.14 Hz.



(b) Mode 2; frequency = 8.58 Hz.

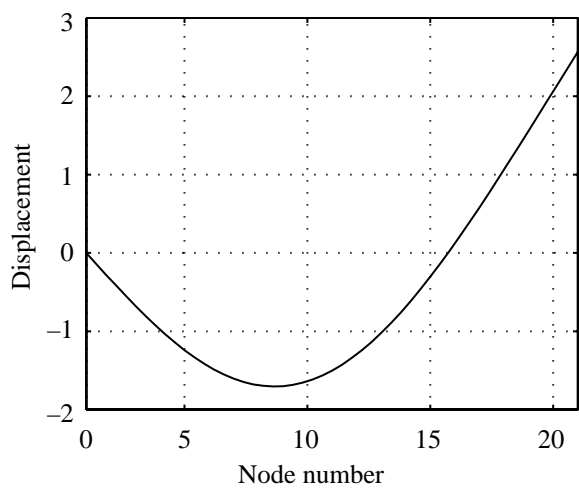


(c) Mode 3; frequency = 19.3 Hz.

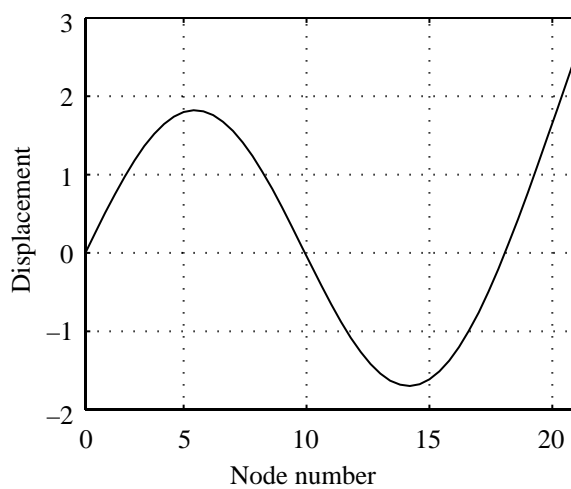


(d) Mode 4; frequency = 34.32 Hz.

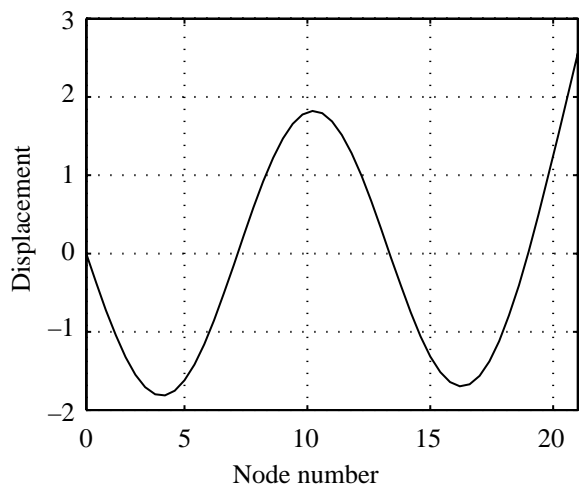
Figure 7. Mode shapes of link 1.



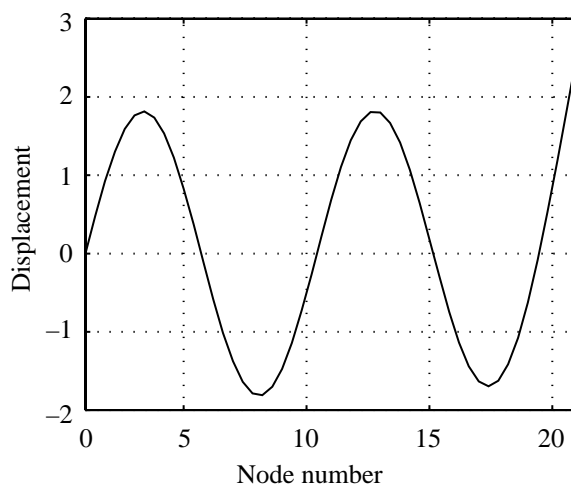
(a) Mode 1; frequency = 3.3 Hz.



(b) Mode 2; frequency = 10.8 Hz.



(c) Mode 3; frequency = 22.5 Hz.



(d) Mode 4; frequency = 38.3 Hz.

Figure 8. Mode shapes of link 2.

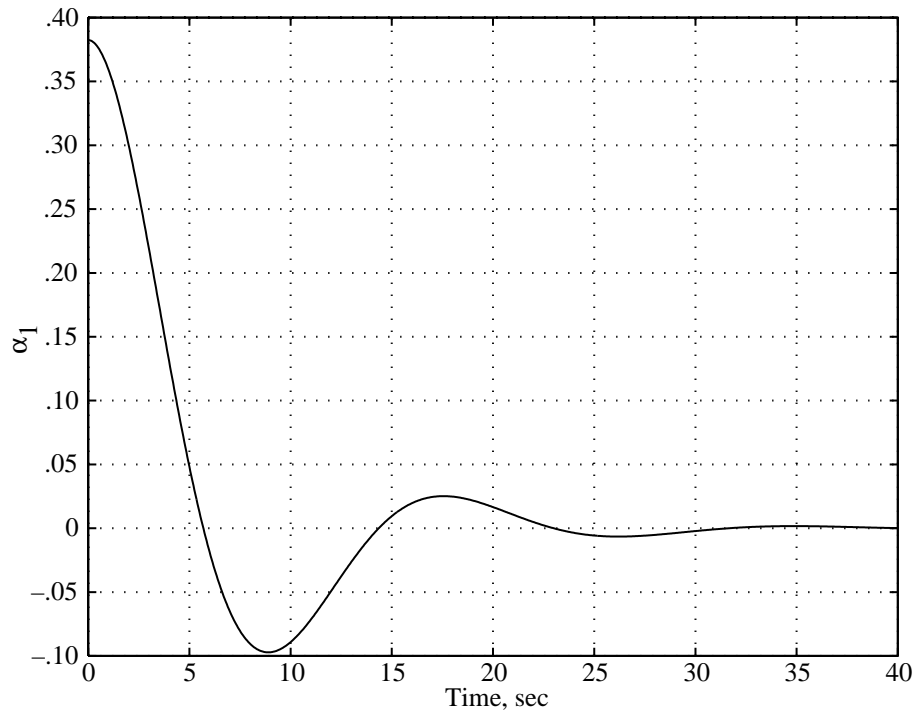


Figure 9. Euler parameter α_1 .

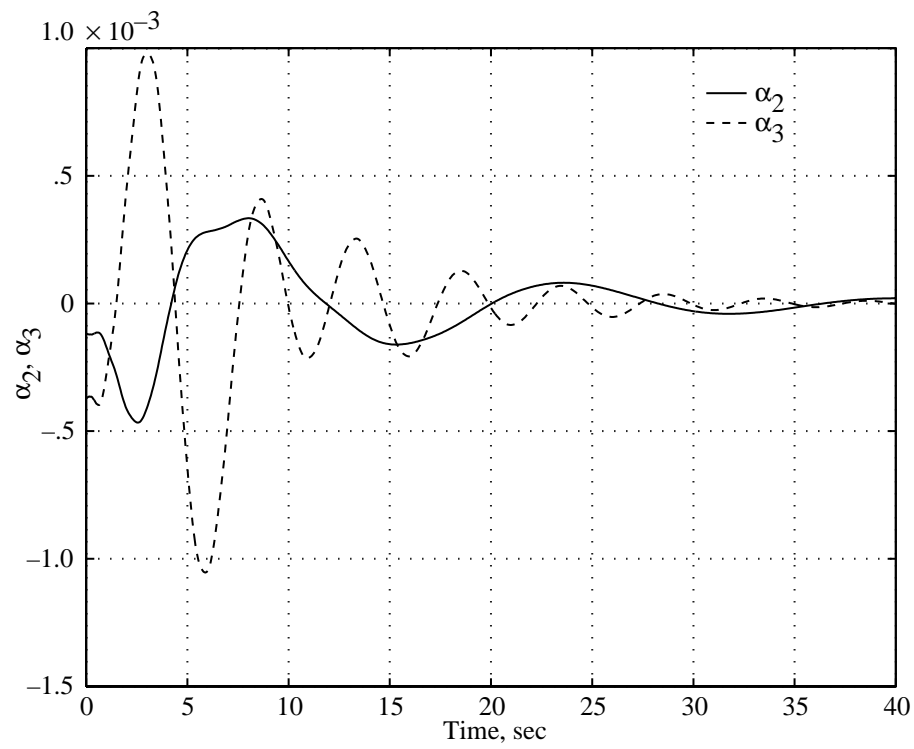


Figure 10. Euler parameters α_2 and α_3 .

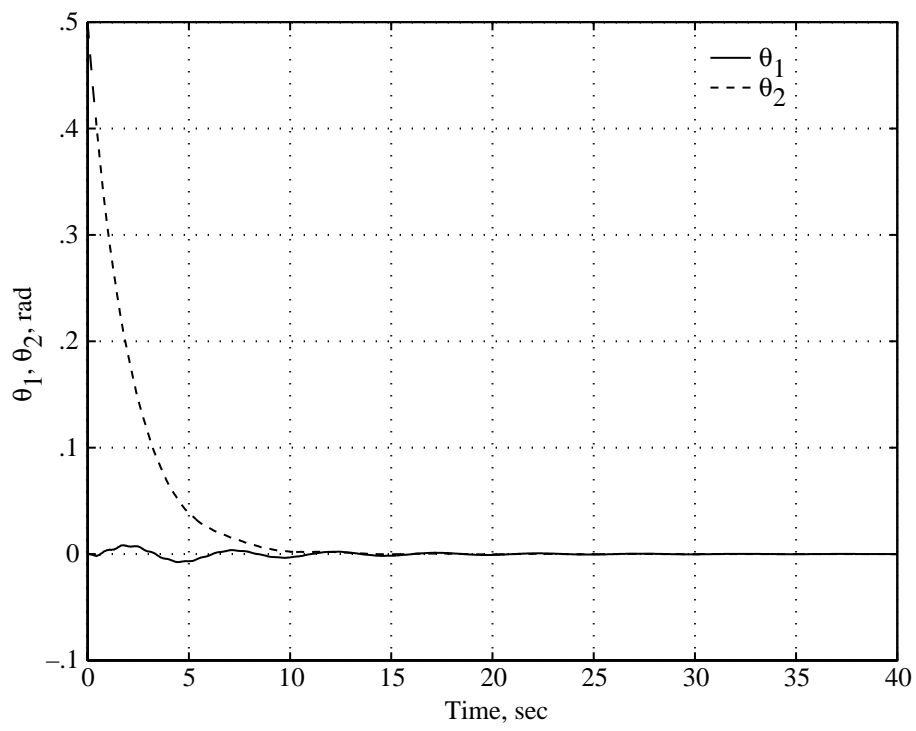


Figure 11. Revolute joint angular displacement.

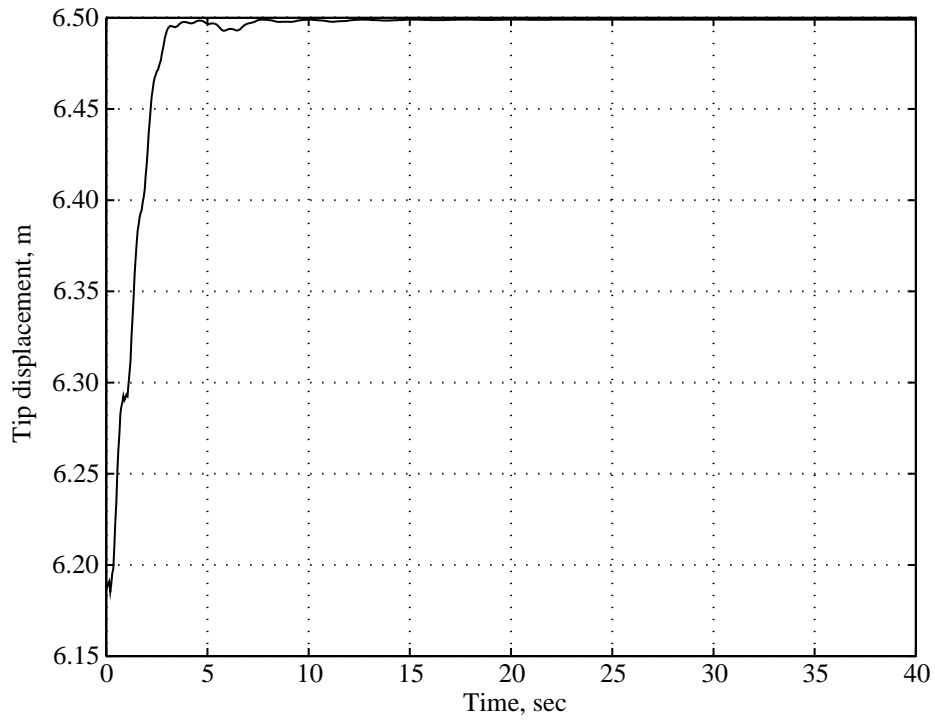


Figure 12. Tip displacement (x coordinate).

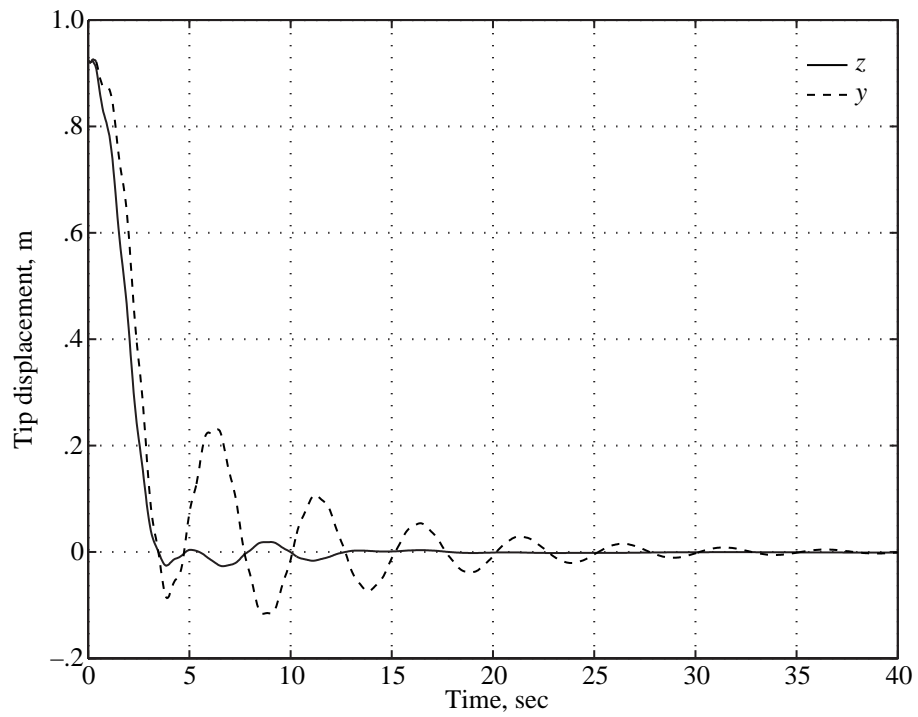


Figure 13. Tip displacement (y and z coordinates).

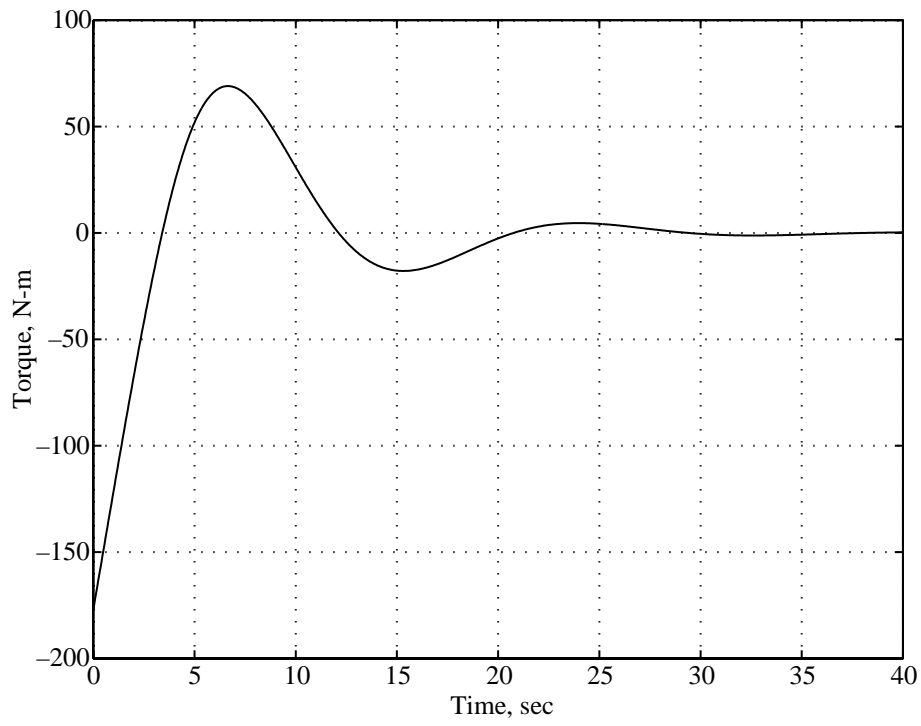


Figure 14. Control torque u_1 .

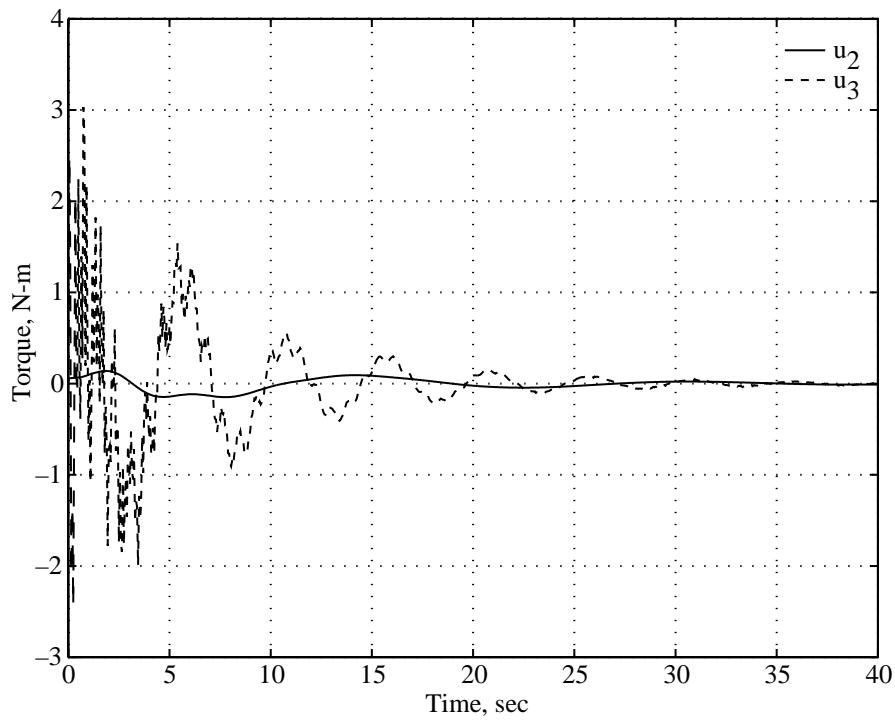


Figure 15. Control torques u_2 and u_3 .

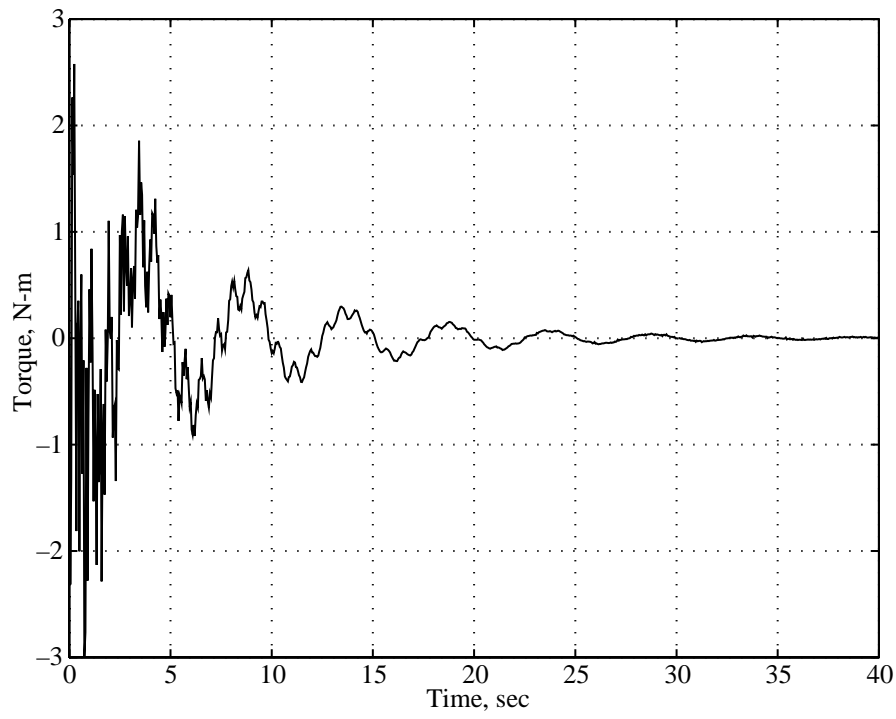


Figure 16. Control torque u_4 at revolute joint 1.

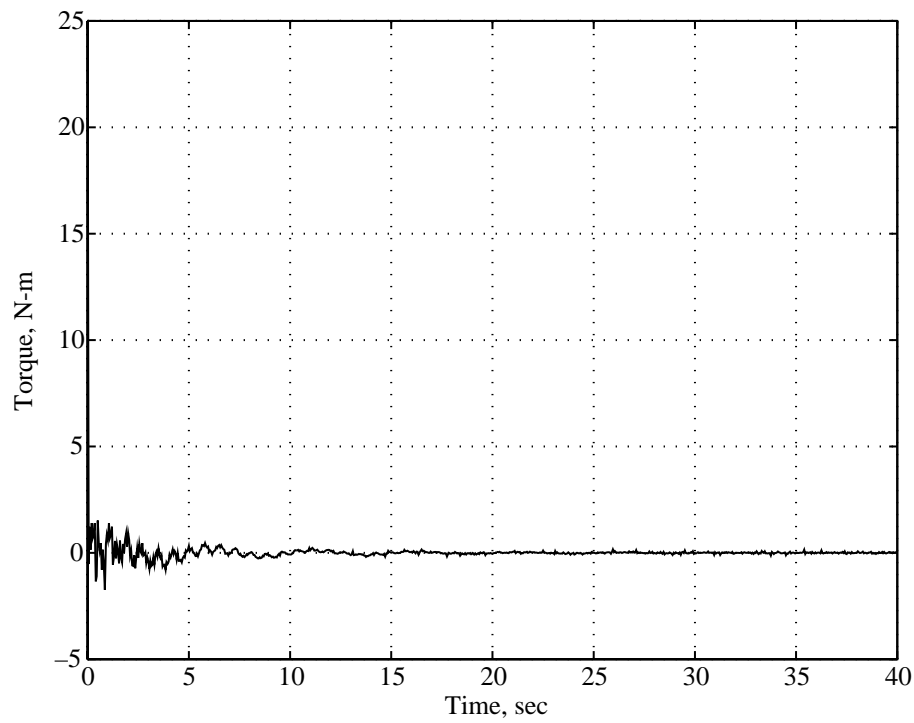


Figure 17. Control torque u_5 at revolute joint 2.

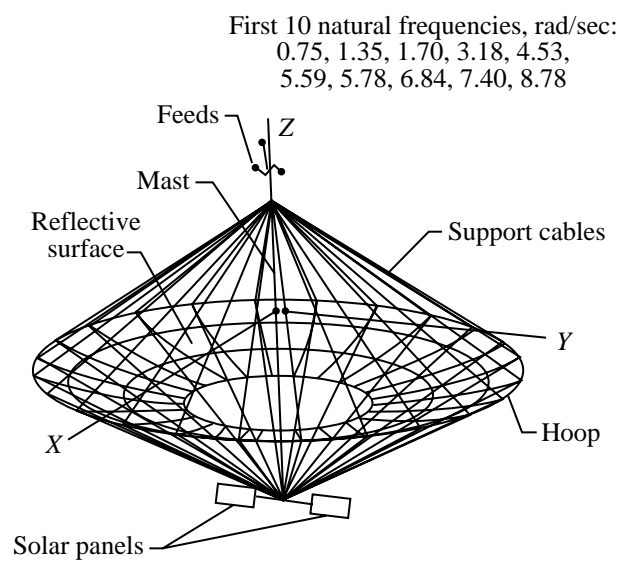


Figure 18. Hoop-column antenna concept.

REPORT DOCUMENTATION PAGE			Form Approved OMB No. 0704-0188	
Public reporting burden for this collection of information is estimated to average 1 hour per response, including the time for reviewing instructions, searching existing data sources, gathering and maintaining the data needed, and completing and reviewing the collection of information. Send comments regarding this burden estimate or any other aspect of this collection of information, including suggestions for reducing this burden, to Washington Headquarters Services, Directorate for Information Operations and Reports, 1215 Jefferson Davis Highway, Suite 1204, Arlington, VA 22202-4302, and to the Office of Management and Budget, Paperwork Reduction Project (0704-0188), Washington, DC 20503.				
1. AGENCY USE ONLY (Leave blank)		2. REPORT DATE May 1995		3. REPORT TYPE AND DATES COVERED Technical Paper
4. TITLE AND SUBTITLE A Class of Stabilizing Controllers for Flexible Multibody Systems			5. FUNDING NUMBERS WU 233-01-01-05	
6. AUTHOR(S) Suresh M. Joshi, Atul G. Kelkar, and Peiman G. Maghami				
7. PERFORMING ORGANIZATION NAME(S) AND ADDRESS(ES) NASA Langley Research Center Hampton, VA 23681-0001			8. PERFORMING ORGANIZATION REPORT NUMBER L-17413	
9. SPONSORING/MONITORING AGENCY NAME(S) AND ADDRESS(ES) National Aeronautics and Space Administration Washington, DC 20546-0001			10. SPONSORING/MONITORING AGENCY REPORT NUMBER NASA TP-3494	
11. SUPPLEMENTARY NOTES Joshi and Maghami: Langley Research Center, Hampton, VA; Kelkar: Langley Research Center (National Research Council Research Associate), Hampton, VA.				
12a. DISTRIBUTION/AVAILABILITY STATEMENT Unclassified-Unlimited Subject Category 18 Availability: NASA CASI (301) 621-0390			12b. DISTRIBUTION CODE	
13. ABSTRACT (Maximum 200 words) This paper considers the problem of controlling a class of nonlinear multibody flexible space systems consisting of a flexible central body to which a number of articulated appendages are attached. Collocated actuators and sensors are assumed, and global asymptotic stability of such systems is established under a nonlinear dissipative control law. The stability is shown to be robust to unmodeled dynamics and parametric uncertainties. For a special case in which the attitude motion of the central body is small, the system, although still nonlinear, is shown to be stabilized by linear dissipative control laws. Two types of linear controllers are considered: static dissipative (constant gain) and dynamic dissipative. The static dissipative control law is also shown to provide robust stability in the presence of certain classes of actuator and sensor nonlinearities and actuator dynamics. The results obtained for this special case can also be readily applied for controlling single-body linear flexible space structures. For this case, a synthesis technique for the design of a suboptimal dynamic dissipative controller is also presented. The results obtained in this paper are applicable to a broad class of multibody and single-body systems such as flexible multilink manipulators, multipayload space platforms, and space antennas. The stability proofs use the Lyapunov approach and exploit the inherent passivity of such systems.				
14. SUBJECT TERMS Multibody systems control; Flexible space structures			15. NUMBER OF PAGES 43	
			16. PRICE CODE A03	
17. SECURITY CLASSIFICATION OF REPORT Unclassified	18. SECURITY CLASSIFICATION OF THIS PAGE Unclassified	19. SECURITY CLASSIFICATION OF ABSTRACT Unclassified	20. LIMITATION OF ABSTRACT	